PARAMETRIC INVESTIGATION OF A THEORETICAL ORGANIC RANKINE CYCLE (ORC)

Investigation of a theoretical ORC system powered by a low-temperature heat stream by varying parameters to evaluate performance and find key performance parameters.

JIM WERNERSSON

School of Business, Society and Engineering
Course: Bachelor thesis energy technology
Course code: ERA 206
Credits: 15hp
Program: Energy technology

Supervisor: Dimitrios Bermperis
Examinor: Maher Azaza
Costumer:
Date: 2023-06-07
Email:
Jim.wernersson@gmail.com

ABSTRACT

The energy resource waste heat or low-grade thermal energy is available in vast quantities. Tapping into this resource and converting it to electrical energy would not only reduce energy waste but also has the potential to eliminate greenhouse gas emissions. One technology developed to utilize this resource is the ORC which uses an organic working fluid that has a low boiling temperature and thus can be vaporized at a low temperature. This work has been focused on evaluating a theoretical ORC system working with a constant net power output of 200 kW and heat source temperature of 80 °C. The assessment was conducted with a model developed within the scope of this work. The model was compared against the literature to ensure more reliable results. Assessment of the system was performed with a parametric investigation to assess how the pinch point temperature difference, Condenser cold fluid inlet temperature, and pressure ratio affect the system performance. For a low-temperature ORC system to achieve good performance the pressure ratio is the most impactful parameter to focus on. However, a low Condenser cold fluid inlet temperature allows for a larger pressure range and increases the system performance for any given pressure ratio. Lowering the cold condenser inlet temperature from 20 to 15 °C provides a large system efficiency gain.

Keywords: ORC, Organic Rankine cycle, parametric evaluation, Waste heat, low-grade temperature, key performance parameters, performance evaluation, auxiliary pumps, system efficiency.

PREFACE

This work has been done to enhance knowledge about how a low-temperature ORC cycle operates and what the key performance parameters are thus providing essential design knowledge. This degree project is written during the energy program at Mälardalen University in Västerås on the twenty sixth of May 2023 and the work corresponds to 15 credits.

Thanks to Dr. Rebei Bel Fdhila for interesting and fruitful initial discussions on the project topic and delimitations. I would also like to thank PhD student Alessandra Ghilardi for providing essential information on the topic and suggestions on how to proceed with the work. And a massive thank you to doctoral candidate Dimitrios Bermperis for excellent guidance and support.

Västerås in June 2023

Jim Wernersson

SUMMARY

Energy is an essential part of both social and economic development. However, a large proportion of the energy used today comes from fossil fuels. To decrease the use of fossil fuels and primary energy used, waste heat energy can be utilized. There are several categories describing waste heat energy such as high, medium, and low-grade heat. This work has focused on low-grade heat which corresponds to temperatures lower than 100 °C. Low-grade heat is available in vast quantities, but it is challenging to exploit this resource due to the small temperature difference to the environment. However, due to the vast quantity plenty of technologies are being developed and refined to convert this low-grade thermal energy into electricity. One of which is investigated in this work, is the ORC system. The work focuses on evaluating an ORC system performance working with a heat source temperature of 80 °C.

The ORC is based on the traditional widely-used Rankine cycle in which the working fluid is water. But pressurized water has a boiling point temperature larger than 100 °C and thus cannot be used for low-temperature heat source applications. The ORC system utilizes an organic working fluid with a high vapor pressure and low boiling temperature even when pressurized. In this work, the working fluid R245fa was used because of it preforming slightly better than other working fluids at low heat source temperatures.

To perform the evaluation a theoretical representation of the system was built in MATLAB. Including all the main components in an ORC, such as the evaporator, the condenser, the turbine, and the pump. Both evaporator and condenser are heat exchangers which transfer thermal energy from a hot to a cold fluid. In the evaporator, the heat transfer is modeled as two sections one where heat is transferred from liquid to liquid and one from liquid to two-phase (boiling). In the condenser, a third section is included in which heat is transferred from a gas to a liquid. The gas-to-liquid section is discarded in the evaporator, considering the working fluid R245fa it's a dry working fluid i.e., the inherent shape of the saturation bell is tilted. Thus, when the saturated vapor is expanded in the turbine the fluid ends up in a superheated phase. This means that the expander does not have to handle condensation which usually limits the performance and thus the fluid is superheated to avoid this phenomena. The expander and pump are turbomachines the pump induces energy into the liquid increasing the pressure and in the turbine energy is extracted from the fluid by expanding the pressurised gas. The isentropic efficiency is utilized do describe performance losses in the pump and turbine. The model was validated against results from the literature to ensure reliable results.

Two cases were conducted with the model to investigate how the parameters: pressure ratio (rc), pinch point temperature difference ($PPTD$), and the cold condenser inlet temperature (T_6) affect performance parameters. Performance parameters such as the thermal efficiency the specific work, and the system efficiency. The system efficiency was introduced in this work to provide a representation of how the system would perform by including the work consumed by the auxiliary pumps i.e., the pumps providing water to the evaporator and the condenser. In case 1 the rc and $PPTD$ was varied and in case 2 rc and T_6 was varied.

The evaluation showed that the parameters $PPTD$ and T_6 has no significant effect on either the thermal efficiency or the specific work of the system. But both impact the system efficiency. Thus, a lower $PPTD$ leads to a better-performing system and a similar trend can be identified by lowering T_6. However, in the case were T_6 was varied a turning point was identified in the system efficiency for a pressure ratio larger than 3.4. Reviewing rc all the performance parameters reacted in a positive matter with an increasing rc. However, the system efficiency got affected in a negative manner when the pressure ratio was so high that the evaporation temperature got close to the heat source inlet temperature (T_8). As a cause of a massive increase in work consumed by pump for the secondary system providing hot water to the evaporator.

To increase the ORC performance for a system utilizing a heat source temperature of 80 °C the PPTD and T_6 should be as small respectively low as possible. Considering rc, this parameter should be maximized to the point just below the pressure ratio causing a steep increase in the secondary mass flow in the evaporator.

CONTENT

LIST OF FIGURES

LIST OF TABLES

NOMENCLATURE

Symbol	Description	Unit
A	Area	m^2
g	Gravitational acceleration	$m/s2$
h	Enthalpy	kJ/kg
$\bar{h}$	Mean convection coefficient	$\frac{W}{m^2 * K}$
$\dot{m}$	Mass flow	kg/s
$\eta_{generator}$	Generator efficiency	$\%$
η_{is}	Isentropic efficiency	$\%$
η_{mech}	Mechanical efficiency	$\%$
η_{system}	System efficiency	$\%$
η_{th}	Thermal efficiency	$\%$
p	Pressure	pa
Q	Heat	kW
Q_{loss}	Heat loss to the environment	$\%$
rc	Turbine pressure ratio	$-$
T	Temperature	K
$T_{h,s}$	Heat source inlet temperature	$°C$
U	Heat transfer coefficient	$\frac{kW}{m^2 * K}$
V	Velocity	m/s
$\dot{W}_{net}$	Net power output	kW
W_p	Pump work	kW
W_{shaft}	Shaft work	J/kg
$\dot{W}_t$	Turbine work	kW
Z	Hight	m
ϵ	Effectiveness (heat exchanger performance)	$[-]$
ρ	Density	$\frac{kg}{m^3}$

ABBREVIATIONS

Abbreviation	Description
cond	condenser
evap	evaporator
hs	Heat source
is	isentropic
p	Pump
PPTD	Pinch point temperature difference
SH	Superheating
spec	Specific work
t	Turbine
wf	Working fluid

1 INTRODUCTION

1.1 Background

Energy is a cornerstone in today's world, it fuels economic growth and social development. This means developing efficient ways to use available energy and thus having more energy at hand can elevate both the economic and the social sector. Investing in energy efficiency also has the benefit of lowering the energy needed and reducing the overall cost of energy purchase (Energy Agency, n.d.).

According to Li et al. (2022), waste heat has over recent years become a more interesting research topic due to the possibility to reduce the amount of primary energy used. If more waste energy could be utilized this will bring both economic and environmental benefits (Li et al., 2023). Jouhara et al. (2018) mention that waste heat could be subdivided into high, medium, and low-grade temperatures, where high-grade temperatures are over 400C°, medium-grade temperature is in the range of 100-400C° and low-grade heat is below 100 C°.

Huo et al. (2022a) note that low-grade thermal energy is available in large quantities, such as waste heat from industrial factories, geothermal sources, and solar energy. This energy is however quite difficult to recover due to a small temperature difference between the heat source and the ambient temperature (Huo et al. 2022a). In another study from Huo et al. (2022b), they highlight that not using this low-grade thermal energy is not only a massive energy waste but also contributes to thermal pollution in the near surrounding. Because of the vast amount of available low-grade heat, the economic and environmental benefits of converting it to electrical energy would be substantial. Several technologies have been developed to exploit this resource and optimize thermal-electrical conversion. According to Huo et al., the system that converts low-grade heat must meet five important standards. 1. The system should be customized to the conversion of low-grade heat and the structure should be both lightweight and uncomplicated. 2. The cost of operation, maintenance, and investment should be low. 3. The technology should provide a stable operating point, heat-to-electricity output, and long cycle life. 4. Deliver a high heat-to-electricity efficiency. 5. Be composed of non-toxic and environmentally friendly materials. Furthermore, Huo et al. state that applications with low-grade temperatures technologies like the organic Ranking cycle and solid thermoelectric materials have a very low heat-to-electricity efficiency (Huo et al. 2022b). However, Kim et al. (2017) showed in a study that even for a very small experimental ORC system with a scroll expander and evaporation temperature of 80C °they were able to achieve a system efficiency of 3 %. In the same study, they also demonstrated that increasing the pressure ratio over the turbine greatly increases the net power output and system efficiency. Hu et al. (2022) point out that the energy source temperature has been an important determining factor as to if the power generation through an ORC can have a viable economy. But also state that the temperature for which a low-grade temperature power generation project can achieve a good economy keeps dropping due to development in the area. Feng et al (2023) conducted a study that utilized machine learning to evaluate the performance of an ORC cycle utilizing the low-grade heat at the heat source, they were able to show an optimum thermal efficiency of 8.85% and a net power output of 2.87 kW.

1.2 Purpose/Aim

Low-grade waste heat is a widely abundant resource that could be utilized to minimize thermal pollution and the use of fossil fuels. One technology developed to utilize low-grade heat is the ORC. To assess how an ORC system should be designed to enhance performance this work has built a model representing a theoretical system. The performance assessment is done by varying different parameters and evaluating how they affect system output. This work will also identify the key performance parameters and perform a sensitivity analysis. The model includes all the main components such as pumps, condensers, evaporators, and expanders. The performance assessment includes the pumping work from both the primary and secondary pumps, not only the primary working fluid pump.

1.3 Research questions

Which are the key performance parameters and how do they affect the performance of the system?

How are the system efficiency and specific power affected by varying input parameters?

Which are the main constraints in the system and how do they limit performance?

1.4 Delimitation

This work has not investigated the economic or environmental aspects of this system due to the scope of this work. The low-grade heat stream temperature has been assumed to be constant at 80C°. Only one working fluid in the ORC system has been assessed the reasoning is described in more detail in section 2.2. This report will focus on the subcritical saturated ORC and not consider different types of ORC such as a superheated cycle or a critical cycle. The subcritical saturated cycle is the most widely used in real-world systems and therefore the most relevant cycle to examine in this work.

2 METHOD

2.1 Ideal Rankine cycle

In this section, the ideal Rankine cycle is analyzed to provide insight into the ORC. If the working fluid flows through all the components without irreversibility, frictional pressure drops and heat transfer with the surrounding and the work in pumps and turbines is isentropic the process can be identified as ideal and hence described by the following equations.

Work produced in the turbine: $W_{turbine} = \dot{m}(h_1 - h_2)[kJ]$ *Equation 1*

Heat transfer in the condenser: $Q_{condensor} = \dot{m}(h_2 - h_3)\ [kJ]$ *Equation 2*

Work consumed by the pump: $W_{pump} = \dot{m}(h_3 - h_4)\ [kJ]$ *Equation 3*

Heat transferred to the working fluid: $Q_{evaporator} = \dot{m}(h_4 - h_5)\ [kJ]$ *Equation 4*

Thermal efficiency: $\eta_{th} = \frac{W_{turbine} - W_{pump}}{Q_{evaporator}}$ *Equation 5*

2.2 Subcritical organic Rankine cycle

The subcritical organic cycle (SORC) is related to the ideal Rankine cycle however in the (SORC) or basic ORC as it is also called. The fluid after the expander may not end up in the two-phase area due to the inherent "bell" appearance of the organic fluid which can be identified in *Figure 1*. When evaluating the SORC non-isentropic pumping and turbine work are considered. But heat transfer to the environment is neglected in the pump and turbine.

The ORC cycle which has been investigated is a subcritical saturated steam cycle, which according to Hu et al. (2022) is the most used cycle in real-world systems to date. The working principle of this cycle is shown in *Figure 1*. The working fluid selected to conduct this test is R245fa which Hu et al. found to be suitable as a working fluid for heat source temperatures between 80-100C°. Providing a slight power advantage over the other working fluids which were examined in their study.

The Organic Rankine cycle starts at the preheater (1-2) where the fluid gets heated to saturated liquid. After the preheater the working fluid enters the evaporator (2-3) where the liquid is heated to saturated steam, the steam is expanded in the turbine (3-4) which produces mechanical work which can be used to drive a generator. From the turbine outlet the fluid is condensed back to a liquid state in the condenser (4-5) the fluid then enters a pump which raises the pressure in the system (5-1). The fluid is then led back to the starting point at the inlet of the preheater.

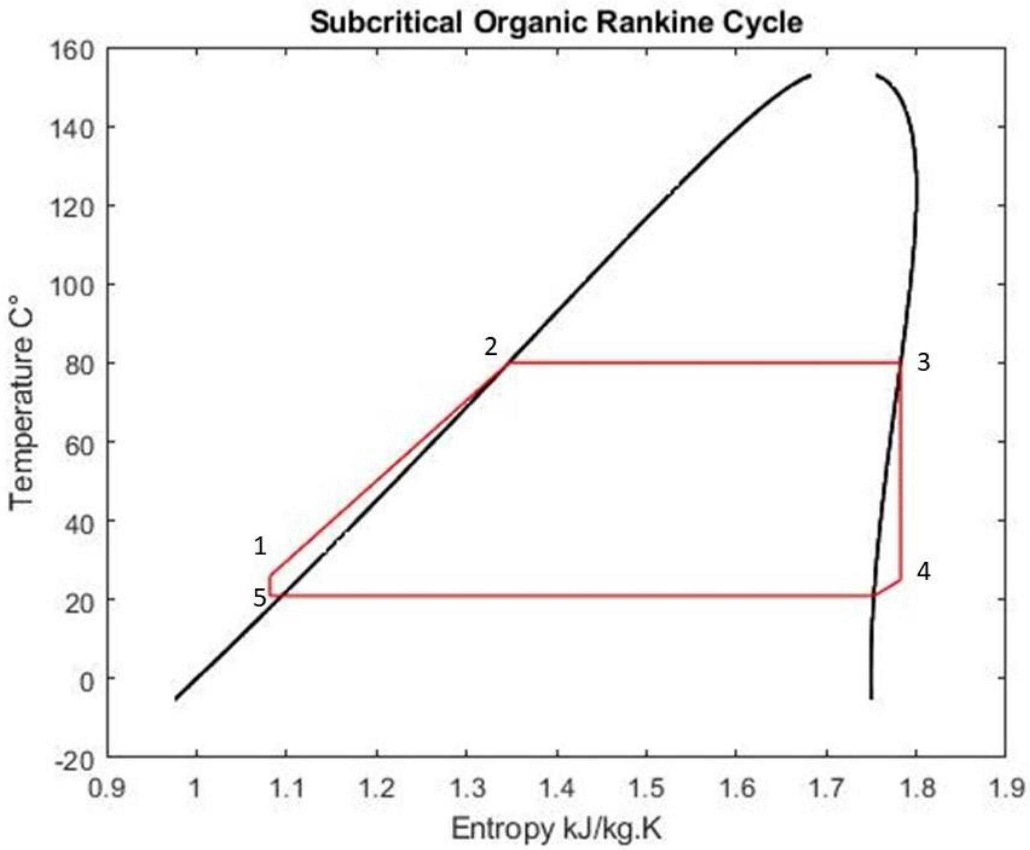

Figure 1 Thermodynamic process over an isentropic subcritical organic Rankine cycle.

2.3 Model

A model in MATLAB has been developed in this work to create a representation of the thermodynamic ORC. MATLAB is a desktop-based programming platform that allows the user to create models, analyze data, visualize data, program scrips etcetera. A model can be created with a script by combining complex functions and equations to make a representation of a real-world system and analyze it in a safe and easy-access environment. Data visualization is useful for showing results and enhancing readability. MATLAB programming language can handle matrix and array mathematics thus effectively handling large datasets. MATLAB also provides a wide variety of built-in functions which speed up the programming process.

MATLAB has been chosen as the model development tool thus it allows for an effortless handling of large data sets. Provide easy access to a large library of functions and assist with programming. The model is comprised of three pumps, two heat exchangers a heat source, and a turbine which is presented in *Figure 2*.

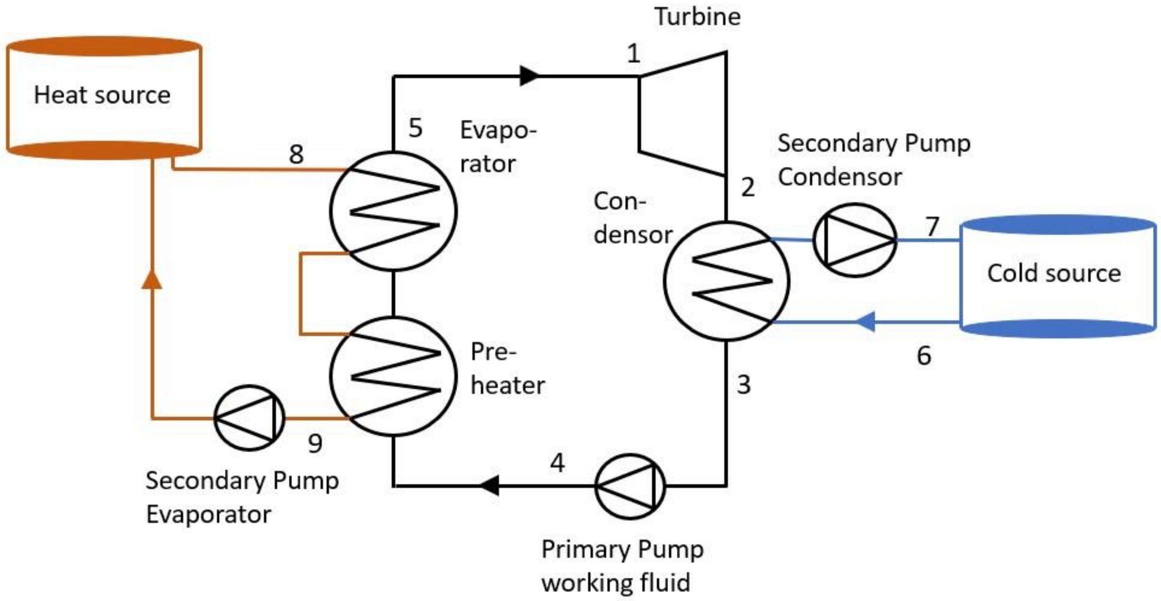

Figure 2 Modell representation.

2.4 Literature and data collection

To access reviewed and contemporary articles about the work performed in this report Scopus has been used alongside Primus and Google Scholar. Some of the search phrases are stated below.

- {Low grade heat} OR {Waste heat} "utilization" OR "potential"
- "ORC" OR "Organic Rankine cycle" "80C" OR "Low-grade heat" OR "low temperature"
- "Low-grade heat" OR "waste heat" AND "electrical power generation"
- "Organic Rankine cycle" OR "ORC" "waste heat" OR "low-grade heat" OR "low temperature" "architectures" OR "configurations"
- "Waste heat" OR "low-grade heat" OR "low temperature" OR "100C" "evaporator" OR "boiler" "organic Rankine cycle" "ORC"

In conjunction with the searches on the above-stated websites, books from libraries at Mälardalens University in Västerås and Malmö University have provided information on components and systems assessed and modeled in this work.

3 THEORETICAL FRAMEWORK/ LITERATURE STUDY

The model development consists of combining theory and equations from different components to create a whole system. In the process of converting heat energy to electrical energy through an organic Rankine cycle a variety of components is combined. The turbine expands the gas and creates mechanical work, the condenser which is used to cool the working fluid to liquid state, the pump which increases the pressure in the system, and the evaporator which transfers heat to the working fluid causing it to boil and evaporate. These above-stated components will be further explained in detail below.

3.1 Pumps

Pumps are hydraulic machines designed to increase the pressure, the potential energy, and/or the kinetic energy of the fluid (Alvares, 2006). They are used in all sorts of applications and sizes large pumps can distribute fluids in a district heating network or small pumps which are used to provide a small dose of liquid. Further Alvares states that energy is either transferred by the centrifugal forces in the impeller and/or the conversion of kinetic energy to pressure by diffusing the fluid, diffusing the fluid leads to a pressure rise in the static- and dynamic pressure. Diffusion of the fluid consumes work in contrast to expansion which produces mechanical work in a turbine. The pump consists of an impeller, housing, bearings, and shaft. To drive the pump the shaft is connected to a motor. There are several pump architectures that are all specialised for a specific case for example centrifugal pumps, axial pumps, reciprocating pumps etcetera. In a study by Yang et al. (2018) working fluid pumps for ORC systems are evaluated and the multistage centrifugal pump seems to achieve the greatest efficiency at outlet pressures in the span of 0.4-1.1 MPa. Centrifugal pumps consist of an impeller which is followed by a diffuser, the fluid gets sucked into the center of the machine entering axially, and the impeller turns the flow path of the fluid by increasing the kinetic energy and whirling it outwards causing the flow to exit radially through the diffusers which convert the kinetic energy in the fluid to pressure energy (Dixon & Hall, 2010). After the flow has passed the diffusers, the flow enters a collection area called a volute which guides the flow onward to the outlet pipe of the pump. When designing a system including a pump cavitation is a phenomenon that is important to circumvent, it occurs when the static pressure of the fluid becomes lower than the vapor pressure of the fluid at the given temperature (Dick, 2010).

3.2 Turbine

The turbine like the pump is also a turbomachine but in contrast to the pump which induces energy into the fluid, the turbine extracts energy from the fluid (Dick, 2022). The energy extracted from the fluid to the shaft can then be used for something useful such as turning a generator and thus generating electricity. The turbine has been developed in different directions to handle different fluids, mass flows, and applications, to mention a couple: the steam turbine, gas turbine, wind turbine, and water turbine are all turbines specialized to extract energy from a certain fluid and fluid state. Dick describes the axial turbine as a collection of stators followed by rotors, a stator is stationary and consists of vanes that prepare the flow to enter the rotor which consists of rotating blades that extract energy from the fluid. How much work is produced in each rotor can be evaluated with Euler's work equation and is strongly related to how much the flow is turned in the rotor. A steam turbine or a vapor turbine expands either superheated vapor or saturated vapor to a low pressure and lower temperature which in some cases cause the fluid to condensate and end up in the two-phase region. When the fluid condensate at the turbine outlet the flow entering the condenser is a mix of vapor and liquid. When a vapor or a gas is used as the working fluid the fluid is compressible and thus when evaluating such a system the theory of compressible flow must be applied. Xia et al. (2018) conclude that the performance of the expander in the ORC is a key component and thus should be optimized. Further Xia et al. identify that for low-grade heat applications radial-inflow turbines are frequently chosen as the expander because of the capability to provide a high efficiency and allow for a large enthalpy drop even though the peripheral velocity is low. However, a study from Naas et al. (2021) investigates the feasibility to utilize a three-stage axial turbine in the ORC system when working with a small mass flow and low-grade heat energy as the energy source. They show that axial turbines can achieve isentropic efficiencies up to 88 % when the turbine is spinning at high rpm (16 000), the isentropic efficiency seems to increase with increasing rotational speed.

3.3 Heat exchangers

The heat exchanger is designed to transfer thermal energy from one fluid to another which is physically separated from one another with a solid wall (Incropera & DeWitt, 2002). The flow arrangement in the heat exchanger usually works as a classification and the simplest form is either a parallel flow or a counterflow heat exchanger. Incropera and DeWitt argue that the counterflow heat exchanger generally has better performance than the parallel flow, but the parallel flow configuration is used when there are constraints to consider which doesn't allow for a counterflow heat exchanger. The design of the heat exchanger is impacted by the fluid states, if the heat exchange is between a liquid and a gas which are not to be mixed fins are usually applied on the gas side to increase the heat exchange rate. To exchange heat between two liquid fluids the shell-and-tube configuration is commonly used as a plate heat exchanger. According to Imran et al. (2015), heat exchangers are an exceptionally important component in nearly all thermal systems and thus the design and choice of exchanger type should be optimized to enhance the system performance.

Both the evaporator and the condenser are heat exchangers (Granryd et al., 2009). In the evaporator, heat is transferred from the heat source to the working fluid causing it to vaporize. During the evaporation of the working fluid the temperature does not change if the pressure is constant which can be seen in *Figure 3,* the x-axis represents the length of the evaporator or condenser thus the area in contact with the working fluid. The evaporator heat source may be a liquid, gas, or solid, however, the latter is rare. In a study by Imran et al. (2015), they investigate the performance of a counter-flow chevron plate heat exchanger working as the evaporator in a low-grade heat ORC system. The plate heat exchanger is subdivided into three sections, section one handles the liquid-to-liquid heat transfer, the second section is liquid two-phase i.e., vapor and liquid mix heat transfer, and the third section is where heat is transferred between liquid and vapor. However, because of the properties of working with R245fa, no superheating is needed and thus, the third section of the heat exchanger is discarded. Imran et al. stress the importance of a pressure drop in the evaporator. Thus, a high-pressure drop will decrease the amount of enthalpy drop in the turbine which leads to a net power loss. The authors also stress that the pressure drop in an evaporator is strongly related to the cost. Thus, a low-pressure drop heat exchanger is more expensive than a high-pressure drop heat exchanger. Furthermore, Imran et al. explain that the pressure drop in a chevron plate heat exchanger has a significant relationship with the heat exchanger area. Thus, a larger heat exchange area led to a higher pressure drop.

In the condenser, heat is transferred from the working fluid to a heat sink which causes the working fluid to condensate back to a liquid state. The heat sink can similarly to the evaporator be either liquid or gas (Granryd et al., 2009). In a study by Kaya et al. (2017), they stress the importance of optimizing the condenser performance. Thus, the condenser has a great impact on the whole ORC system efficiency. Further Kaya et al stress that if the condenser area is too small all the vapor and liquid mix exiting the turbine isn't condensed which can cause damage to the other components included in the system.

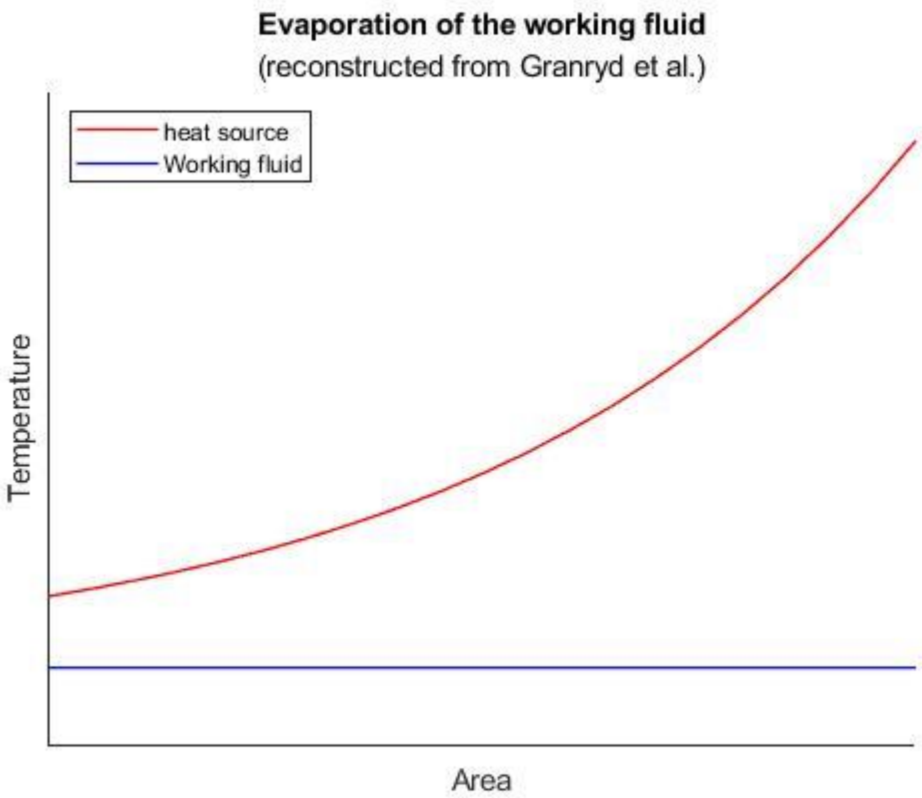

Figure 3 Evaporation of the working fluid.

3.4 Organic Rankine cycle

The ORC is based on the Rankine cycle which uses water as the working fluid (Jouhara et al., 2018). However, the organic Rankine cycle uses a different working fluid, an organic fluid with a low-temperature boiling point and high vapor pressure. Jouhara concludes that this property allows the ORC cycle to utilize low-temperature waste heat as the energy source to generate electricity. The main working components in the ORC are a pump, evaporator, turbine, and condenser. The organic gas gets heated in the evaporator to superheated gas and expands through the turbine creating mechanical work which can be converted to electrical energy through a generator. At the turbine outlet, the gas is led to the condenser where it gets cooled back to a liquid state, and from the condenser the fluid gets pumped back to the evaporator. The ORC can use a wide pallet of working fluids that are suitable for different temperatures and system sizes, Jouhara stresses the importance of choosing a working fluid, thus not optimizing the working fluid could lead to an overall efficiency loss of up to 6%. Even though ORC systems are already installed and in use Lecompte et al. (2015) suggest that the need for improving cost-effectiveness still exists. According to Lecompte et al., there are five important design parameters to consider when optimizing an ORC which is: 1) working fluid should be properly selected, 2) hardware that is suitable for the application, 3) control and optimize system operation, 4) The individual component layout, and 5) sizing of the components. Further Lecompte et al. state that minimizing the irreversibility in the system is key to maximizing the performance, they also stress that exergy efficiency is an appropriate performance indicator. In an article from Hu et al. (2022) the performance of a subcritical ORC cycle working with five commonly used working fluids and a low-temperature energy source is evaluated. To see which of the working fluids has the most promising performance when working with a heat source temperature between 80-100C°. Hu et al. conclude that the performance difference between the working fluids chosen for the comparison is not significant when optimizing for power output per unit weight of water from the energy source. However, they note that the working fluid R245fa has a small advantage providing a higher power output than the other fluids. Further Hu et al shows that the pumping power needed varies a lot for the different fluids with R113 performing the best and R600a the worst. The same study from Hu et al. also shows that the optimal evaporation temperature of the working fluid is slightly lower than the temperature of the heat source. According to Wang et at. (2020), the most suitable working fluid for low temperatures when optimizing for minimal greenhouse gas emissions is R601, and if the optimization was set to minimize the economic aspects R245fa performed the best. In a study by Kim et al. (2017) where an ORC system is examined by experimental tests with a scroll expander. The authors show that for a system that utilizes a temperature of 80C° in the evaporator to vaporize the working fluid R245fa. The cooling fluid entering the condenser must be lower than 30C° for the system to achieve a positive system efficiency. Thus, stressing the importance of the heat sink temperature in systems utilizing low-grade heat in the evaporator. In the same study, Kim et al experimentally show that the pressure ratio over the turbine is an important performance indicator, increasing the pressure ratio leads to higher torque from the turbine and thus a higher power output and higher system efficiency. Kim et al identified that a higher-pressure ratio increases the power consumption of the pump but when the pressure ratio surpasses 2 the power output from the turbine exceeds the power consumed by the pump, which means that the system becomes a net power producer. In the same study by Kim et al., they investigated how varying the mass flow rate of the working fluid between 15-45 g/s at a given temperature and keeping the pressure constant would impact the system performance. They showed with an increasing mass flow rate the rate of absorbed energy in the fluid increased. Increasing the mass flow rate also led to a higher evaporation pressure which further increased the absorbed heat in the working fluid. Kim et al. also stress that the increased mass flow rate of the working fluid increased the power consumed by the pump however, the increased mass flow accelerated the expander and thus led to higher net power output.

3.5 R245fa

Working fluid R245fa is a dry working fluid which means that the slope is positive as can be identified in *Figure 4*. So, when the fluid is expanded from the saturated vapor point the fluid does not end up in the two-phase area and thus superheating is not needed when using R245fa as a working fluid in the ORC (Imran et al., 2015).

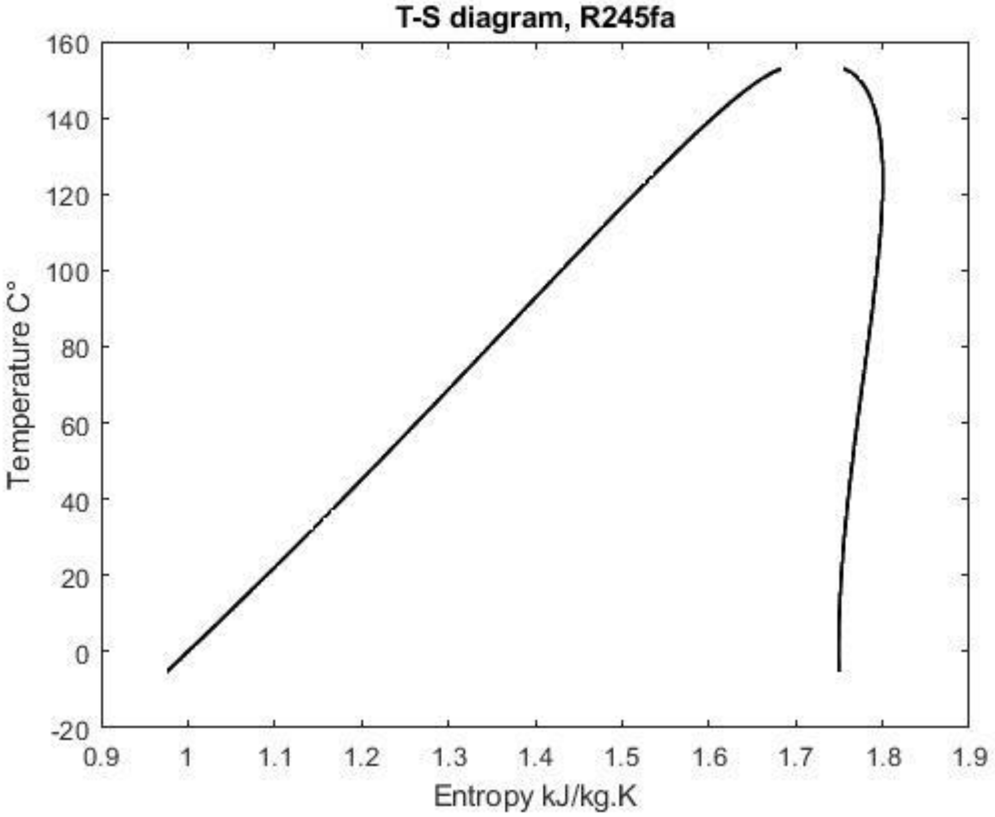

Figure 4 T-S diagram, saturation bell R245fa.

3.6 Other heat-to-electricity conversion technologies

Systems that convert thermal power to electrical power without the step of converting the thermal power to mechanical power first are called direct electrical conversion devices (Jouhara et al., 2018). Technologies such as thermoelectric, piezoelectric, thermionic, and thermo photo voltaic fall into this category. Jouhara explains that examples of implementation of these technologies are scattered in the industry, but some of these technologies have in real-world tests shown promising performance.

Huo et al. (2022b) propose that electrochemical thermoelectric conversion is suitable for a temperature range between 30-90 C°. Huo claims that electrochemical technologies tick a majority of the five standards mentioned in the background and have therefore attracted a lot of attention in the research community. Several electrochemical systems are being researched such as Thermally Regenerative Electrochemical Cycles (TREC), Thermo-Electrochemical Cells (TEC), Thermally Regenerative Ammonia Batteries (TRAB), and Direct Thermal Charging Cells (DTCC). Thermoelectric devices can generate an electrical current when the semiconductor material they are created from gets subjected to a temperature difference between two surfaces (Jouhara et al., 2018). Jouhara affirms that Piezoelectric Power Generation (PEPG) technology can convert low-grade heat directly into electricity with thin-film membranes by utilizing vibrations. Further Jourhara states that these devices have not yet been commercialized due to high manufacturing costs and the complexity of designing a system that is reliable and stable enough to be used in power generation. Jouhara concludes that the operation of thermionic generators has many similarities with thermoelectric devices. But they operate through thermionic emission between the emitter and collector which is subjected to a temperature difference, the emitter to the hot side and the collector to the cold side. Jouhara states that this technology is limited to high-grade temperatures and is not very efficient. The thermo photo voltaic (TPV) generator converts thermal energy to electricity by combining a solar photovoltaic (PV) panel with an emitter and a radiation filter. Jouhara explains that when the emitter is heated from the thermal energy it emits radiation which gets filtered to ensure that only radiation that can be converted to electrical energy passes through and hits the PV panel. According to the author this technology has in some tests shown good heat-to-electricity efficiency results. But an increase in PV cell temperature lowers the radiation conversion efficiency of the PV panel.

Some direct conversion technologies have achieved interesting conversion results, but most of the above-stated technologies are far from being deployed in commercial applications. However, there is a lot of interest in these technologies and their potential, so a lot of research and development is conducted. These technologies might be able to achieve a better heat-to-electricity conversion efficiency than the ORC system in the future however due to a low technology readiness level compared to the ORC they are not further assessed in this work.

4 CURRENT STUDY

In this section, the components and development of the model are described in more detail. Also, assumptions and other constants are stated and discussed. The model station numbers are expansion 1-2, condensing 2-3, compression, 3-4, evaporation 4-5, and in the secondary system 6-7 cooling water condenser and finally 8-9 hot water evaporator.

4.1 General assumptions and constants

Table 1 General assumptions and constants.

General assumptions and constants:		
Variable:	**Value:**	**Unit:**
$Subcooling$	5	K
Q_{loss}	5	%
T_8	353	K
$\eta_{is,t}$	70	%
$\eta_{is,p}$	60	%
$Delta\ p, water\ pumps$	1	bar
$\eta_{generator}$	98	%
η_{mech}	99	%
W_{net}	200	kW

T_8 is restricted to 353 K, which is the outlet cooling flow temperature of a high voltage direct current substation (HVDC) information on the temperature was derived from discussions at Hitachi Energy with R. B. Fdhila (personal communication, March 23, 2023). Subcooling has been set to 5 K to be sufficiently low for the pump to work properly without the risk of cavitation. Heat losses to the environment have been assumed to be 0 in the turbine and pump, but for condenser and evaporator heat losses to the environment have been set to 5%. The isentropic efficiency for the pump and turbine has been set to 60 respectively 70 % which Imran et al (2015) suggested in their study. These isentropic efficiencies were chosen in this work because they represent off-the-shelf components that are supported by values presented in a study by Deethayat et al. (2016). Who used experimental data to validate their model. Isentropic efficiencies suggested by (Xia et al., 2018) are for a theoretical radial-inflow turbine designed for an ORC operating with a low-grade heat source. More values for isentropic efficiencies are provided in *Table 2*. For the water pumps providing hot and cold water to the evaporator respectively condenser. The pressure difference between the inlet and outlet has been assumed to be 1 bar which should be sufficient to provide circulation.

The outlet pressure of the turbine is kept constant, and the inlet pressure is determined by the outlet pressure and the pressure ratio (rc). The pinch point temperature is the temperature difference between the hot fluid and the cold fluid at the closest point in the heat exchangers, which is shown in *Figure 5*. The enthalpy increase when compressing a liquid is very small at low pressures, all the pressures used in this work are <8 bar. Thus, the enthalpies for water and the R245fa have been interpolated with the saturated temperature as input at the state of saturated liquid. Cp for R245fa is used at the temperature of 25 C ° for liquid and for vapor phase 25 °C and 1 atm. Cp for water is interpolated with the mean temperature between inlet and outlet temperatures in each section of the heat exchangers.

The scope of this work does not require a complex model which is why in a similar matter as Hu et al (2022) the system model has been simplified with the assumptions stated below.

- Each component operates in a steady state.
- Pressure losses caused by friction losses in each component and pipes connecting components are ignored.
- Heat loss to the environment is only considered in heat exchangers and heat generated in components are ignored.
- Both the kinetic energy and potential energy of the system are ignored.

4.2 Data

Property data for R245fa has been retrieved from two different sources to include a wider range of saturation temperatures (*R-245fa Is a Hydrofluorocarbon HFC, Refrigerant*, n.d.; *Refrigerant Product Range - TEGA*, n.d.). Data for specific heat capacity for water at constant pressure was downloaded from (*Water (Data Page) - Wikipedia*, n.d.). Property data for water in liquid and vapor state was collected from (Moran et al., n.d.).

Values for a given property that was not exactly presented in the tables were linearly interpolated between the two closest points with a built-in function in MATLAB called "interp1" which works on the same principle as *eq. 6*. But the built-in function also allows "x" to be an array.

$$\frac{x-x_2}{x_1-x_2} = \frac{y-y_2}{y_1-y_2} \qquad \textit{Equation 6}$$

4.3 Condenser

As can be identified in *Figure 5* the condenser model has been divided into 3 sections to model heat exchange between water and superheated gas, water and a mix of liquid and vapor, and water and liquid. Both the condenser and the evaporator have been modeled as a counter-flow configuration. The outlet and intermediate temperatures $T_{h2,3}$ and $T_{c2,3}$ are calculated together with the secondary cooling mass flow and the total heat transferred. Heat loss to the environment is set to 5% for both the condenser and the evaporator. The cooling water mass flow is calculated with an iterative process, where a sufficient Q from the cold source needs to be provided so $T_{h,3} - T_{c,3} = pinch\ point\ temperature$ is achieved at this point the correct secondary mass flow of the condenser is found. Inputs for the condenser are the primary mass flow $\dot{m}_{wf}$ and the inlet temperatures $T_{h,4}$ and $T_{c,1}$, the PPTD and the outlet pressure from the turbine p_4. The outlet temperature from the turbine $T_{h,4}$ is interpolated with the outlet enthalpy from the turbine in a table containing superheated properties. However, before interpolation starts the temperature is crosschecked against the saturated temperature to ensure it's superheated at the pressure p_2. To calculate the intermediate temperatures and the heat transferred from the cooling water the energy balance $eq.\ 7$ was used but no work is produced or consumed so, W=0. For each section of the condenser, the intermediate temperatures can be calculated by combining $eq.\ 7$ and $eq.\ 9$ and adding Q_{loss}. The total heat transferred in the condenser is calculated by adding the heat transferred from each section which is shown in $eq.\ 8$. The subcooling temperature in the condenser is the temperature difference between $T_{h,2} - T_{h,1} = subcool$. Subcooling the saturated liquid is done to avoid boiling in the pump, which induces energy into the fluid. This means that if a flow enters the pump at a saturated temperature there is a high risk of cavitation which can cause damage to the pump and efficiency losses (Alvares, 2006).

In a study from Brodal et al. (2023) where they investigate how to design the best heat exchanger scheme by modeling a heat exchanger focusing on the PPTD and the Thermal conductance (UA). The authors state that heat exchangers operating with $PPTD = 0$ are theoretically optimized. But also mentions that if PPTD is 0 the heat exchange area required for a given heat transfer rate becomes very large. Thus, PPTD can be described as a bottleneck for a heat exchanger and can be directly related to the heat exchange area and the cost.

The relationship between PPTD and the heat exchange area can be noticed by evaluating Newton's law of cooling *eq. 7*. The mean convection coefficient ($\bar{h}$) is a constant so, when the temperature difference becomes very small the area needs to increase to achieve the same amount of heat transfer rate. To achieve a large heat total heat transferred for a small temperature difference the mass flow also needs to increase $\dot{Q}_{tot} = \dot{m} * q$.

$q = \bar{h} * A_s * (T_s - T_\infty)$ *Equation 7*

$0 = Q - W + m(h_{in} - h_{out})\ [J]$ *Equation 8*

$Q_{tot} = Q_{condensation} + Q_{superheat} + Q_{subcool}$ *Equation 9*

$Q = \dot{m} * Cp * (T_{in} - T_{out})$ *Equation 10*

p_2

.

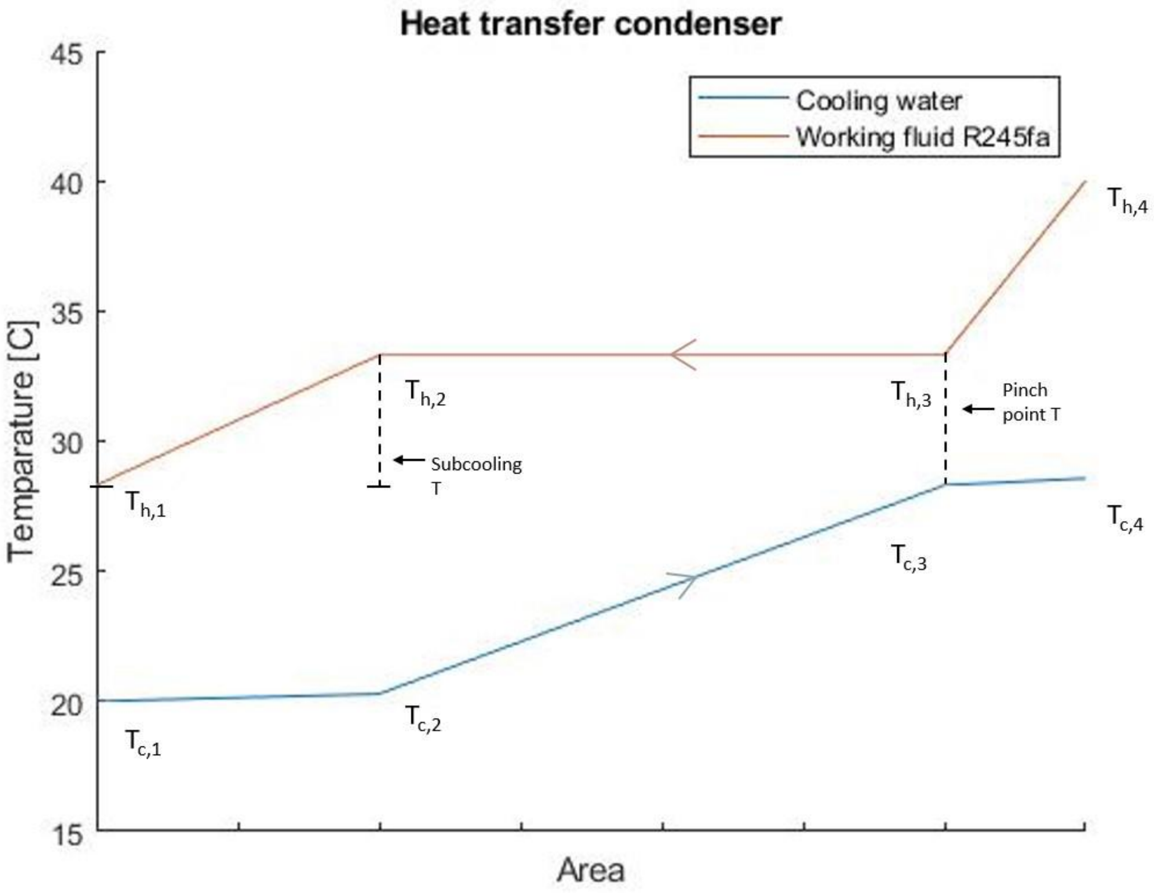

Figure 5 Working principal condenser.

4.4 Evaporator

Like the condenser, the evaporator is divided into sections. However, when modeling the evaporator only two sections are needed, because this work is evaluating a subcritical saturated cycle. So, heat transfer occurs between two liquids in the preheating section and between a liquid and a fluid in the two-phase region in the evaporation section. The inputs to calculate the secondary mass flow in the evaporator are the inlet temperatures $T_{h,3}$, $T_{c,1}$, $\dot{m}_{p,wf}$ and $PPTD$. The intermediate temperature $T_{h,2}$ can be calculated by utilizing $Q_{preheat}$ and similar procedure as described in section 4.3, $T_{h,3}$ is calculated with the same principle as $T_{h,2}$. $\dot{m}_{s,evap}$ is in a similar matter as in the condenser iterated using the $T_{h,2} - T_{c,2} = PPTD$ as a target value.

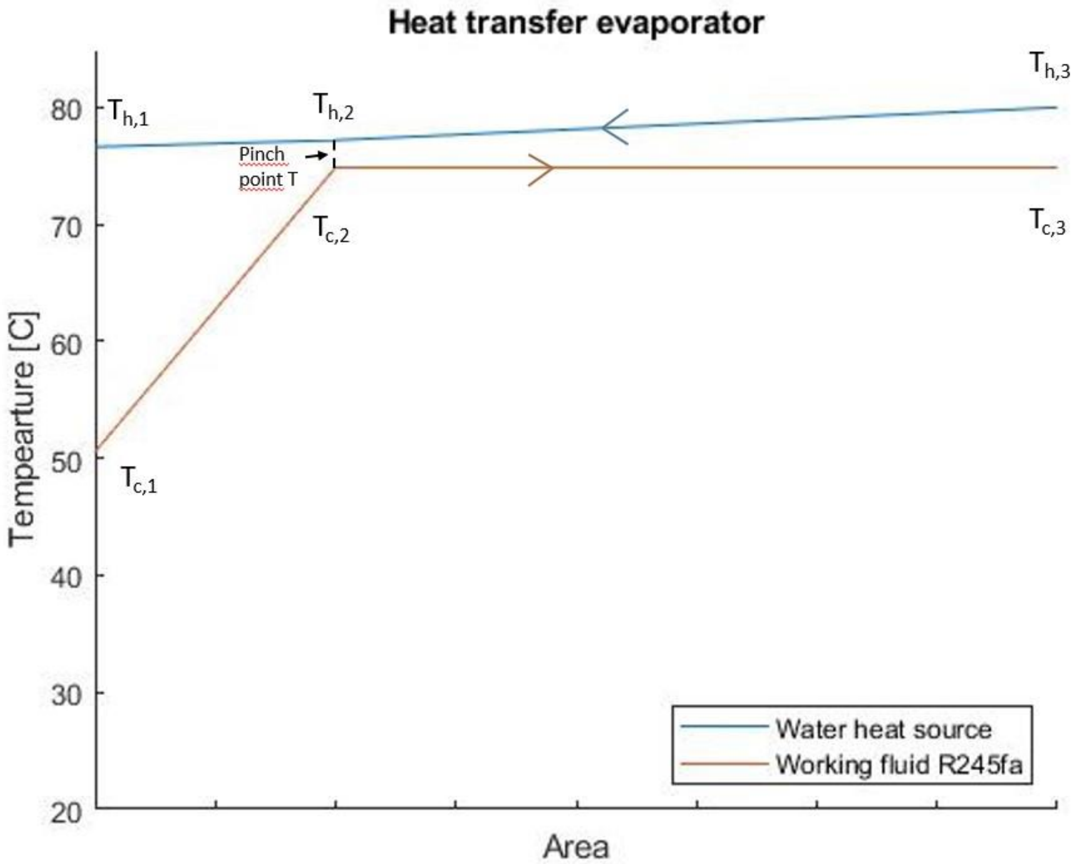

Figure 6 Working principal evaporator.

4.5 Pumps

The extended Bernoulli's equation (*equation 10)* has been used to describe the work consumed by the pumps (Gerhart et al., 2017). Which is suggested to solve problems involving incompressible fluids. Assuming that fluids are incompressible when in a liquid state is according to Alvares (2006) a valid assumption to make.

Losses in *eq. 10* are expressed as in the unit of J/kg but in this work, the isentropic efficiency has been used to include losses for both the pump and turbine. The isentropic efficiency is a ratio between the ideal work needed to increase the pressure to a given pressure if the pump is working adiabatically and without friction. and the actual work needed to achieve the same pressure (Gerhart et al., 2017).

All the pumps modeled in this work are considered to produce a negligible increase in the fluid velocity between the inlet and outlet. The height difference has also been assumed to be zero, the height difference in the real-world system would not be large and thus the added work would be negligible compared to the work needed to achieve the increase in pressure. The working fluid pressure ratio is an input of the model. Thus, the work consumed by the Working fluid pump varies with the pressure ratio. The isentropic efficiency applied in the pump model is set to 60%. The density used to calculate the consumed work by the pumps is interpolated from table values.

$$\frac{p_{out}}{\rho} + \frac{V_{out}^2}{2} + gz_{out} = \frac{p_{in}}{\rho} + \frac{V_{in}^2}{2} + gz_{in} + Wshaft - loss \; [J/kg] \qquad \textit{Equation 10}$$

$$w_{pump} = \frac{\frac{p_1}{\rho} - \frac{p2}{\rho}}{\eta_{is,p}} \; [J/kg] \qquad \textit{Equation 11}$$

4.6 Turbine

The work produced in the turbine can be calculated by combining the mass and energy balance at a steady state can be calculated with *eq. 8*. If the process is assumed to work adiabatically, without friction losses, and the isentropic efficiency *eq. 8 is* reduced to *equation* 12. Inputs used to calculate the turbine work was p_1,rc,$\dot{m}_{p,wf}$. p_1 was used to interpolate the saturated temperature T_1 and with T_1, $S1$ could be interpolated. Assuming isentropic expansion $h_{2,is}$ could be interpolated by utilizing with S_1 and p_2. To find the actual h_2 the definition of isentropic efficiency was used (*eq. 13*). As described in section 3.5 R245fa is a dry working fluid which means that when expanded in the turbine the fluid at the turbine outlet is at a superheated state. The outlet temperature was interpolated with p_2 and $h_2$using a table including properties at a superheated state. To find the actual work which the turbine needs to produce to achieve the net power output W_{net} *eq.12* is combined with the isentropic efficiency, mechanical losses, and generator efficiency to get *eq. 14*. $W_{t,electrical}$ is the electrical power output produced by the turbine, but some power is consumed by the auxiliary components i.e., the pumps. Thus, the net power output from the system is equal to the intermediate power produced by the turbine $W_{intermidiate}$ *eq. 16*. So, for the system to produce sufficient output power $\dot{m}_{p,wf}$ is iterated to find the correct value and *eq. 16* is used as the target. This means that for each iteration of $\dot{m}_{p,wf}$ the secondary mass flows are iterated and thus the power consumed by the pumps gets updated before a new wave of iterations starts.

$$\dot{W}_t = \dot{m}_{p,wf}(h_{in} - h_{out}) \; [kW] \qquad \textit{Equation 12}$$

$$\eta_{is} = \frac{h_{out} - h_{in}}{h_{out,is} - h_{in}} \; [-] \qquad \textit{Equation 13}$$

$$W_{t,electrical} = W_t * \eta_{generator} * \eta_{mech} * \eta_{is,t} \qquad \textit{Equation 14}$$

$$W_{intermediate} = W_{t,electrical} - W_{p,wf} - W_{s,cond} - W_{s,evap} \qquad \text{Equation 15}$$

$$W_{net} = W_{intermidiate} \qquad \text{Equation 16}$$

Isentropic efficiency model results and experimental results from the literature are presented in *Table 2*. With the data presented below the isentropic efficiencies for the turbine were set to 70 % as Imran et al. (2015) used in their study. These seem to be reasonable efficiencies for off-the-shelf components which is supported by the isentropic efficiencies presented by Deethayat et al. (2016) where they used data from a real-world system to validate their model.

Table 2 Isentropic efficiencies collected from literature evaluating the ORC system or individual components.

Authors:	Net power: [kW]	Turbine power [kW]	η_{is} Pump: [%]	η_{is} Turbine: [%]	Heat source temp: [K]	Turbine inlet temp: [K]	η_{th} Thermal efficiency: [%]
Li et al. 2023	29.55		70	80	448		12.8
Deethayat et al. 2016	16	20		71.4	389		
Deethayat et al. 2016	16	20		67.9	381		
Deethayat et al. 2016	16	20		56.6	370		
Saleh et al. 2007	1000		65	85		373	≈12.5
Imran et al. 2014	74		60	70	363		
Xia et al. 2018	595		75	78–81		353–373	

4.7 Organic Rankine Cycle

To evaluate the performance of the system the thermal efficiency *eq. 17* is calculated and the system efficiency *eq.18*. The thermal efficiency excludes isentropic efficiencies and is calculated assuming isentropic components. However, to get a more accurate estimation of how much of the thermal energy gets converted to electrical power this work has included another term of efficiency *eq. 18*. This includes the isentropic efficiencies of all the components and the work consumed by all the pumps.

$$\eta_{th} = \frac{\frac{\dot{W}_t}{\dot{m}} - \frac{\dot{W}_p}{\dot{m}}}{\frac{\dot{Q}_{in}}{\dot{m}}} \qquad \textit{Equation 17}$$

$$\eta_{system} = \frac{\dot{W}t - \dot{W}_{p,R245fa} - \dot{W}_{p,condensor} - \dot{W}_{p,evaporator}}{\dot{Q}_{evaporator}} \qquad \textit{Equation 18}$$

$$W_{t,spec} = \frac{\dot{W}_t - \dot{W}_{p,wf}}{\dot{m}_{wf}} \qquad \textit{Equation 19}$$

4.8 Conducted cases.

The cold source inlet temperature T_6 was in case 1 chosen at the normal mean temperature of the Västerås area over 1 year (*Normal Årsmedeltemperatur | SMHI*, n.d.).

For case 2 T_6 was varied between 278 K and 293K. 293 K is the mean day temperature between May and September and should therefore correspond to the system operating during summer. The PPTD is an important parameter when designing a heat exchanger thus it greatly affects both size and heat transfer rate. There is an optimal PPTD value for a given set of fluids and temperatures. However, finding the optimal PPTD value was beyond the scope of this work. Brodal et al. (2023) conducted a case study to find the best heat exchanger schemes, the PPTD, and the thermal conductance were important parameters to adjust to achieve good heat exchanging performance. For 6 cases they found that PPTD values between 5-16K achieve a good heat transfer rate with a given set of temperatures pressures and fluids.

To investigate how a low and a more reasonable PPTD would affect the ORC system performance the PPTD range was set in this work to 2-10K. For case 1 p_2 has been set to 1.3 bar, lower pressures lead to expansion to the two-phase area. The upper limit of the pressure ratio is confined by the evaporation temperature which is interconnected to the inlet pressure of the evaporator. For case 2 p_2 is confined by the upper limit temperature of T_6, the upper limit of the pressure is however not as restricted due to a smaller pinch point temperature thus max $p1$ for case 2 is 6.7 bar.

Table 3 Case 1 inputs

Case 1 inputs		
T_6	278	K
rc	1.5-4.5	-
p_1	1.95-5.85	Bar
p_2	1.3	Bar
PPTD	2-10	K

Table 4 Case 2 inputs

Case 2 inputs		
T_6	278-293	K
rc	1.5-3.7	-
p_1	2.7-6.7	Bar
p_2	1.8	Bar
PPTD	5	K

5 RESULTS

The results achieved in this work are presented below in two cases. For case one the pinch point temperature difference and the pressure ratio are varied. In the second case, the pressure ratio and the condenser cold inlet temperature are varied.

5.1 Comparison with literature

To ensure that the model developed within the scope of this work produces reliable results it should be validated against results found in the literature. However, a full validation was beyond the scope of this work. Thus, a comparison was performed comparing the thermal efficiency with results from the literature. The calculated thermal efficiency was compared to model results achieved by Canbolat et al. (2023) with a slight deviation. However, it is important to note that in a study by Canbolat et al, an internal heat exchanger was implemented in the system to reuse some of the heat left in the working fluid after exiting the turbine to heat the working fluid coming out from the pump before entering the evaporator. The evaporation pressure deviates slightly between this work and Canbolat et al. The evaporation pressure used in this work is the saturated pressure at the given temperature T_{evap}. The relative deviation between the thermal efficiency calculated in this work and the thermal efficiency which Canbolat et al presented in their study is 6% and the absolute deviation is 0.9 %.

Compared to data set 2 produced by Zare, V. (2015) the relative deviation is 5 % and the absolute 0.8 % when comparing the thermal efficiency of the system. However, in the study by Zare, V. the working fluid was superheated by 4 °C before entering the turbine. In the example created in this work to validate the performance of the model, the superheating was set to 0 due to a lack of data at 27 bars for a superheated state. However, when comparing enthalpy at 25 bars deviation between 0 degrees of superheating and 5 degrees of superheating the enthalpy change is 10 kJ/kg and should not affect the results much.

As both Canbolat et al. and Zare, V. (2023; 2015) the thermal efficiency in this work has been calculated with *eq. 17*.

Scaling the net power output from a large system which was modeled in Zare, V.'s (2015) study to the size used in this work is not an issue. The thermodynamics of different system sizes remain the same. Large systems real-world systems usually incorporate components specifically designed for the system while smaller systems usually use off-the-shelf components with slightly weaker performance. Thus, the efficiencies of individual components will not be as good as in larger systems.

Table 5 Inputs and output for comparing the model.

	Comparison data set 1	**Comparison data set 1**	**Comparison data set 2**	**Comparison data set 2**
	(Canbolat et al., 2023)	This work	(Zare, 2015)	This work
$Fluid$	R245fa	R245fa	R245fa	R245fa
T_{evap} $[°C]$	128	128	135	135
p_{evap} $[bar]$	22.54	22.61	27.01	27.01
T_{cond} $[°C]$	40	40	40	40
$PPTD$ $[°C]$	10	10	10	10
$SH[°C]$	-	-	4	0
$W_{net}[kW]$	-	200	2840	2840
$\boldsymbol{\eta_{thermal}}$ [%]	**15.2**	**14.3**	**14.6**	**15.4**

5.2 Case 1, varying the pressure ratio and the pinch point temperature.

All The graphs in this section were comprised by alternating the $PPTD$ and rc in the system while $W_{net,}p_4, T_{6,} T_8$ and $Subcooling$ is kept constant. rc affect the inlet pressure of the turbine and $PPTD$ affect the secondary intermediate and outlet flow temperatures in the evaporator and condenser. For a low-pressure ratio, the system is a net power consumer. When the pressure ratio is larger than 1.1 the system efficiency becomes positive, and the system is a net producer of electricity. This differs from the experimental results stated by Kim et al. (2017) where a pressure ratio of 2 was needed before the system became a net producer.

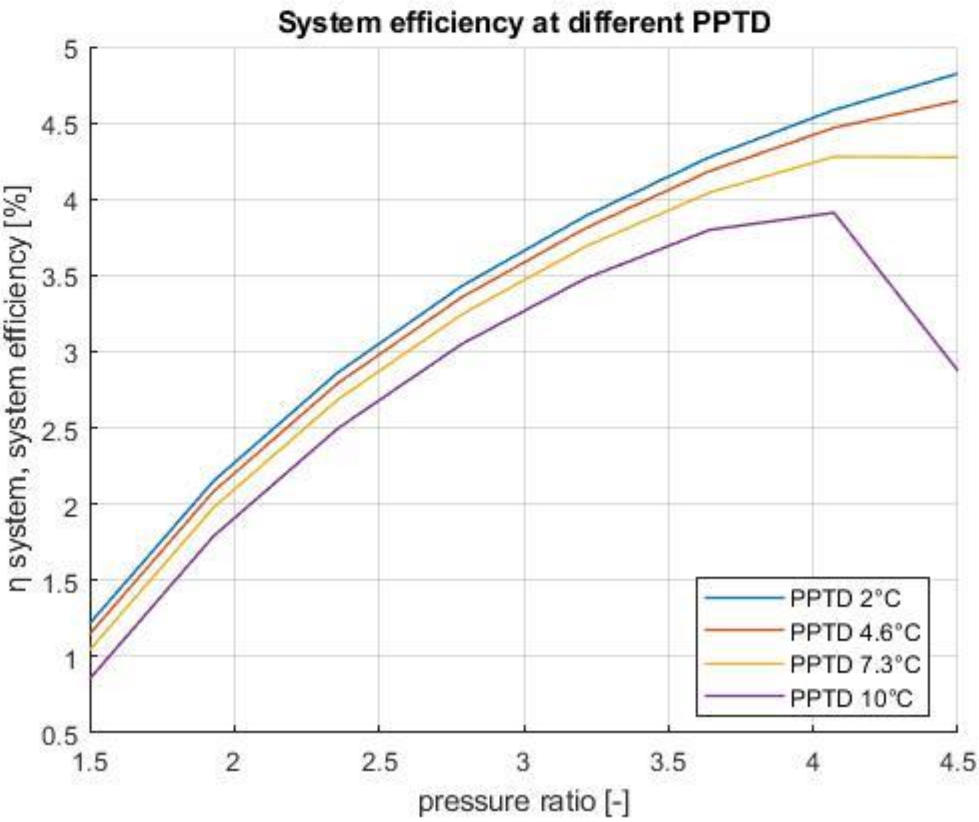

Figure 7 System efficiency at different PPTD and pressure ratios.

The system efficiency is affected positively with an increasing rc and a decreasing $PPTD$ as shown in *Figure 7*. For a low-pressure ratio, the $\dot{m}_{p,wf}$ which is iterated for each wave of inputs that need to increase to keep $\dot{W}_{net}$ constant. If $\dot{m}_{p,wf}$ increases, more fluid needs to be heated or cooled in the heat exchangers. Causing an increase in the secondary mass flows for the system to achieve the correct working fluid outlet temperatures, which can be identified in *Figure 10,11*. The secondary mass flow increase is more prominent in the condenser because of a smaller temperature difference between T_6 and T_2. Contrary to the evaporator where there is a large temperature difference between T_8 and T_4 because of the low evaporation temperature which corresponds to rc. When $PPTD$ is set to 10 °C the system efficiency reaches a turning point when rc is 4, and the system efficiency in this point is 4%. It is however important to notice that the resolution of the graph is not accurate enough to see if this is the actual maximum system efficiency, thus the actual maximum can be between a pressure ratio of 4 -4.5. This suggests that for lower $PPTD$ the turning point of the η_{system} is found at a higher rc when the evaporation temperature $T_{evap} - (T_{hs} - PPTD)$ converges towards 0. However, when evaluating the turning point η_{system} the effect of $\dot{W}_{spec}$ also need to be considered. Because of the growth of $\dot{W}_{spec}$ with increasing pressure ratio. With a decreasing $PPTD$ the system efficiency increases, it is however important to note that for a high system efficiency when decreasing the $PPTD$ a penalty must be paid in heat exchanger size and cost. Why the system efficiency decreases with a higher $PPTD$ can be identified by reviewing *Figure 11* in which the $\dot{m}_{s,cond}$ increases with an increasing $PPTD$ thus affecting the $\dot{W}_{s,cond}$ to increase.

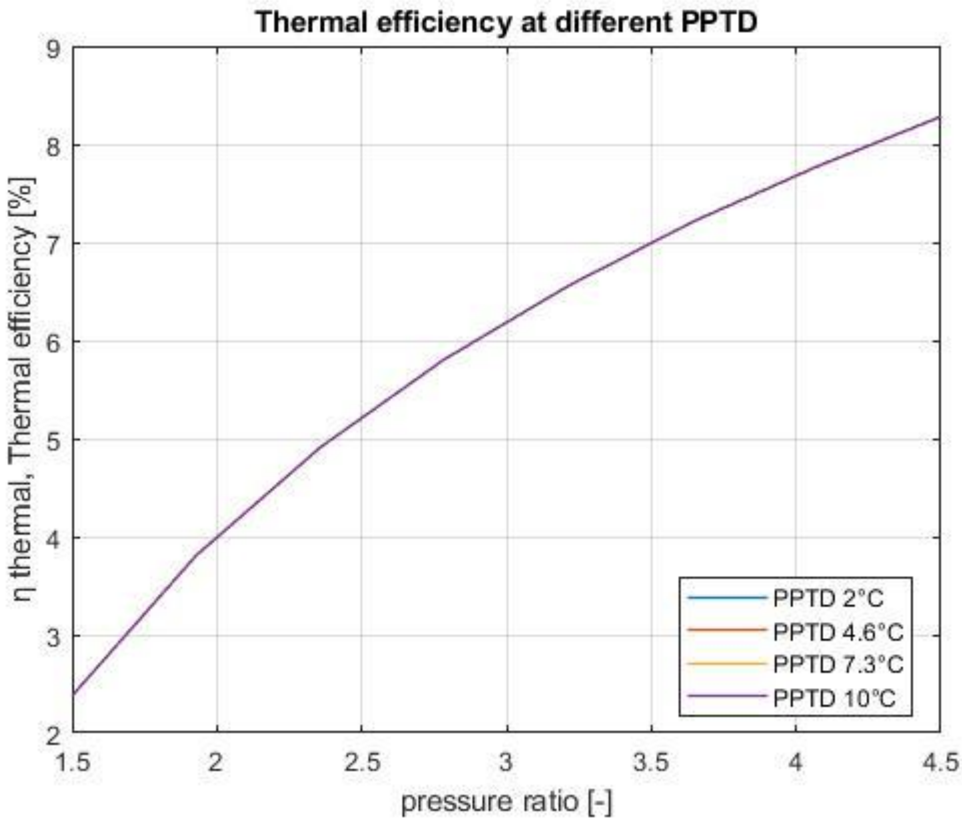

Figure 8 Thermal efficiency at different PPTD and pressure ratios.

When comparing the η_{th} to η_{system} the system efficiency is about 3% lower than the thermal efficiency, which means that almost half of the useful power output is consumed by the secondary pumps. This can be explained by analyzing the equations for η_{th} and η_{system}. The thermal efficiency only includes the work consumed by the primary pump and not the work consumed by the secondary pumps nor the isentropic efficiency of the components. Which the system efficiency does and thus a lower efficiency is identified in the system efficiency. Both efficiencies increase for an increasing rc, but for the system efficiency, there is a trend change when the pressure ratio is larger than 4 and PPTD is 10. For the thermal efficiency the trend of increasing seems to be intact with an increasing rc, nor does it seem to be affected by the PPTD.

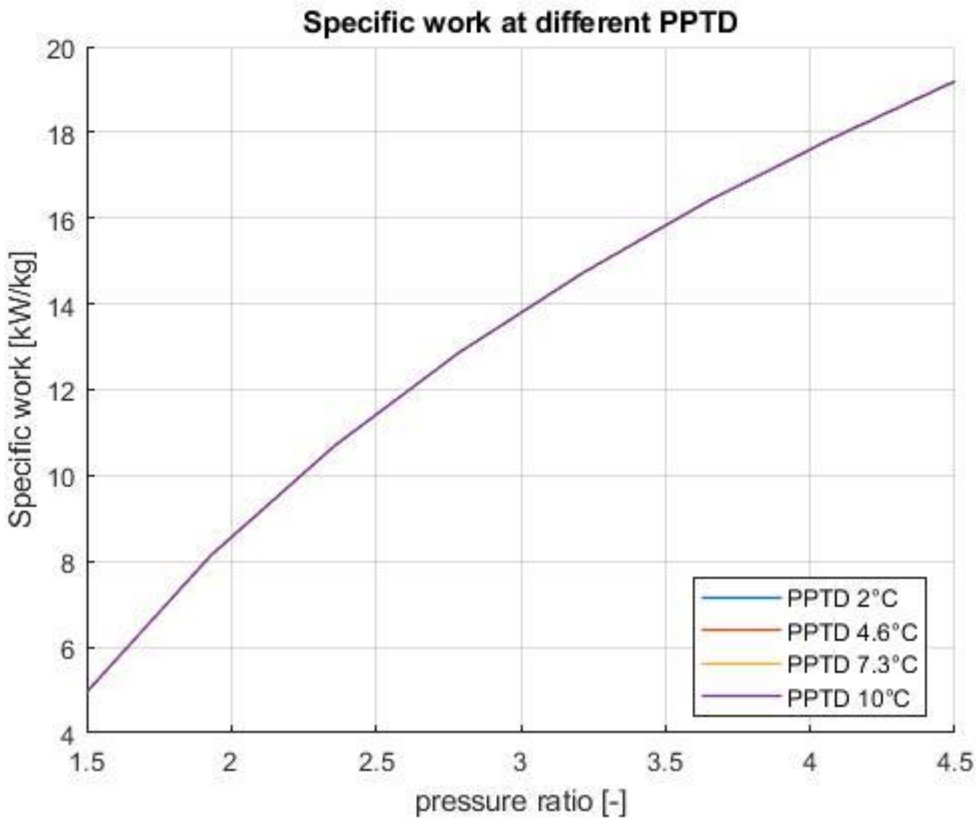

Figure 9 Specific work at different PPTD and pressure ratios.

The specific work plotted in *Figure 9* shows that varying $PPTD$ does not affect the specific work. This can be identified by evaluating equation 19, only including the primary pump and the work produced by the turbine. The increase in rc affects the specific work output in a positive matter. Thus, a smaller system could be achieved by increasing the pressure ratio to be as large as the constraints from the evaporator and condenser allow. In the shape of evaporation temperature and condensing temperature which are both interconnected with pressure.

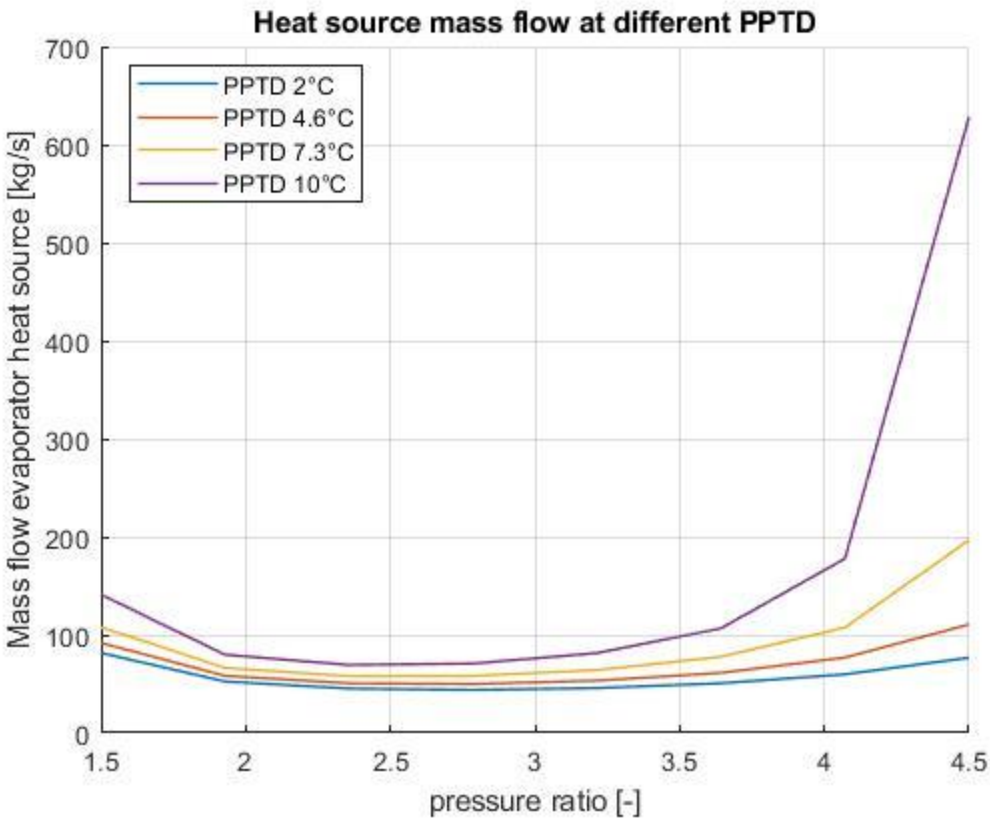

Figure 10 Evaporator secondary mass flow at different PPTD and pressure ratios.

When analyzing the secondary mass flow in the evaporator the lowest point is in a pressure ratio between 2-3.5. A larger mass flow between 1.5 and 2 can be explained with a low specific power output at a low-pressure ratio thus more working fluid is needed to achieve the net power output. But when the pressure ratio is larger than 3.5 the secondary mass flow increases dramatically, especially for the PPTD 7.3 and 10 °C. This can be explained by evaluating the evaporation temperature at the high-pressure ratios. A larger pressure ratio led to a high evaporation temperature and thus, a small temperature difference to the T_8. As explained in more detail under section 4.3 a small temperature difference led to a high mass flow and thus more $\dot{W}_{s,evap}$ which needs to be compensated by an increase in the primary mass flow.

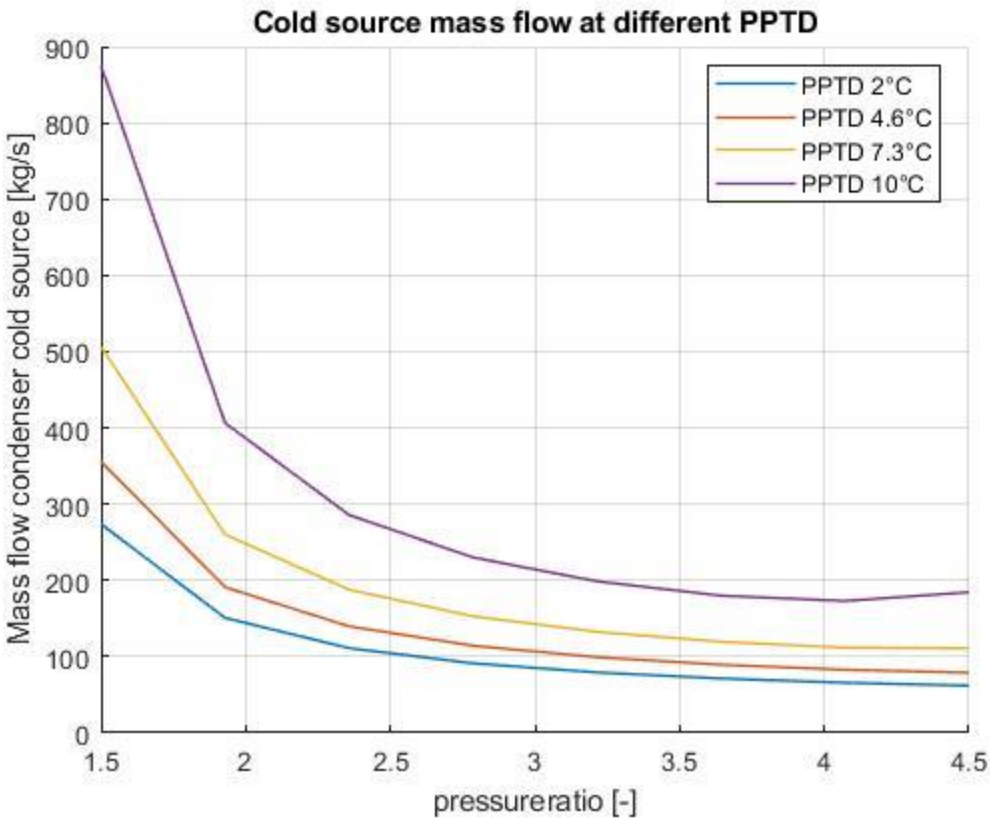

Figure 11 Condenser secondary mass flow at different PPTD and pressure ratios.

Figure 11 shows that for an increasing pressure ratio the $\dot{m}_{s,cond}$ keeps decreasing for all PPTD except 10 °C. For this case, a turning point is found between rc 4-4.5. When reviewing *Figure 10* an increase in $\dot{m}_{s,evap}$ is clear from rc 2.5 and onwards, but when rc reaches the value of 4 the mass flow increases dramatically. This means that for rc between 2.5-4, the specific work output of the system increases faster than the increasing $w_{p,evap}$. For $PPTD$ <10 °C the decrease in $\dot{m}_{s,cond}$ can be explained by reviewing *Figure* 9 which shows that the $\dot{W}_{spec}$ increases with an increasing rc. Thus, less working fluid is needed to produce the same amount of $\dot{W}_{net}$ which affects the $\dot{m}_{s,cond}$ in a positive manner. It is however difficult given the results to see if the mass flow in the condenser will keep dropping if the pressure ratio is increased even more. *Figure 10* suggests that the $\dot{m}_{s,evap}$ will dramatically increase with an increasing rc because the evaporation temperature will at a point come very close to T_8. Causing a similar effect as seen in the example PPTD 10 °C.

5.3 Case 2, varying the pressure ratio and the inlet condenser temperature.

All The graphs in this section were comprised by alternating the T_6 and rc in the system while W_{net}, p_4, $PPTD$, T_8 and $Subcooling$ is kept constant. rc affect the inlet pressure of the turbine and T_6 is the secondary inlet temperature in the condenser. Note that the pressure ratio in case 2 does not correspond to the same inlet pressures as used in case 1, inputs for case 2 are summarized in *Table 5*. For case 2 PPTD is set to 5°C.

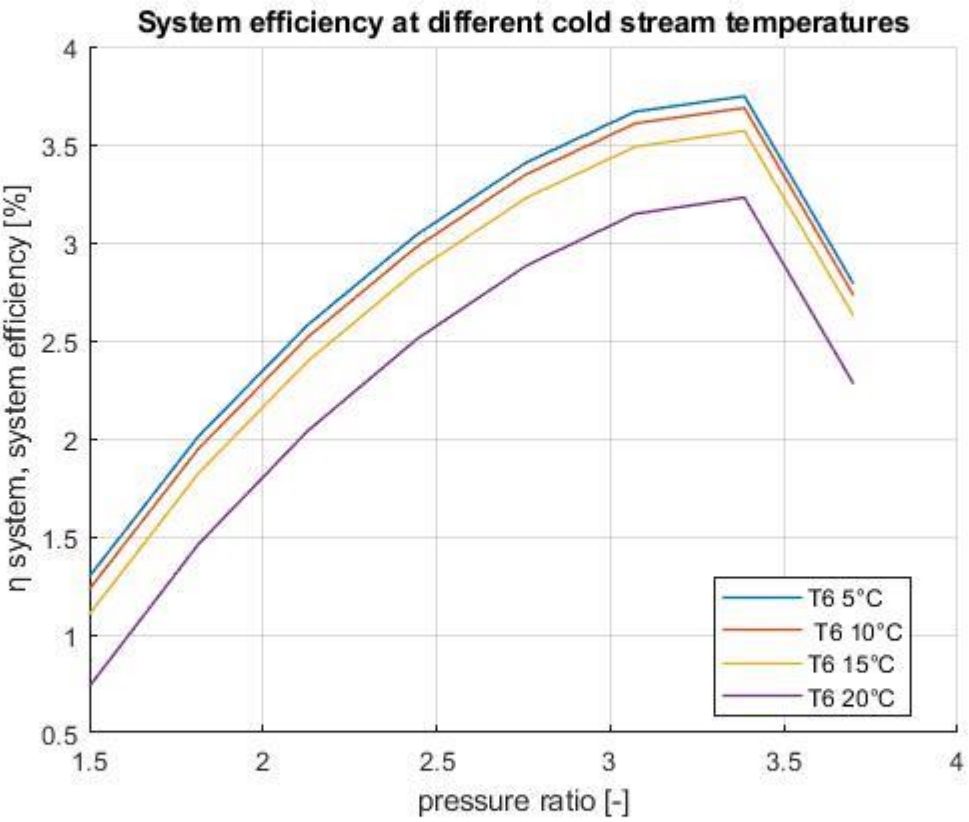

Figure 12 System efficiency at different T6 and pressure ratios.

Figure 12 clearly shows that a lower condenser inlet temperature has a positive effect on the system efficiency leading to a higher system efficiency at any given point. The increase in system efficiency between the two lines appears to be constant. Thus, the distance between two lines at a given point seems to be the same along the whole length of the lines. The increase in efficiency for a lower T_6, can partially be explained by reviewing *Figure 16*. Where $\dot{m}_{s,cond}$ increases with a higher T_6, however, in *Figure 16* no parallelism between the lines can be identified. The benefit of decreasing T_6 is reducing with a decreasing T_6, the largest system efficiency increase in observed when T_6 is decreased from 20 to 15 °C. This might be explained in *Figure 16,* where a similar trend can be identified. All curves in *Figure 12* encounter a turning point at some point after the pressure ratio of 3.4. the resolution of the curves is too low to identify the optimum. But the rapid decrease in system efficiency after rc 3.4 can be explained by analyzing *Figure 15* which shows a rapid increase in $\dot{m}_{s,evap}$ after rc 3.4. The rapid increase in $\dot{m}_{s,evap}$ led to high power consumption by the secondary pump which must be compensated by a mass flow increase primary cycle. The increase in $\dot{W}_{s,evap}$ increases so fast that the otherwise positive effect on the system efficiency caused by specific work when rc increases is overruled. It is possible to identify that the system can convert thermal energy to electrical energy with the highest efficiency at a rc between 3.4 and 3.7.

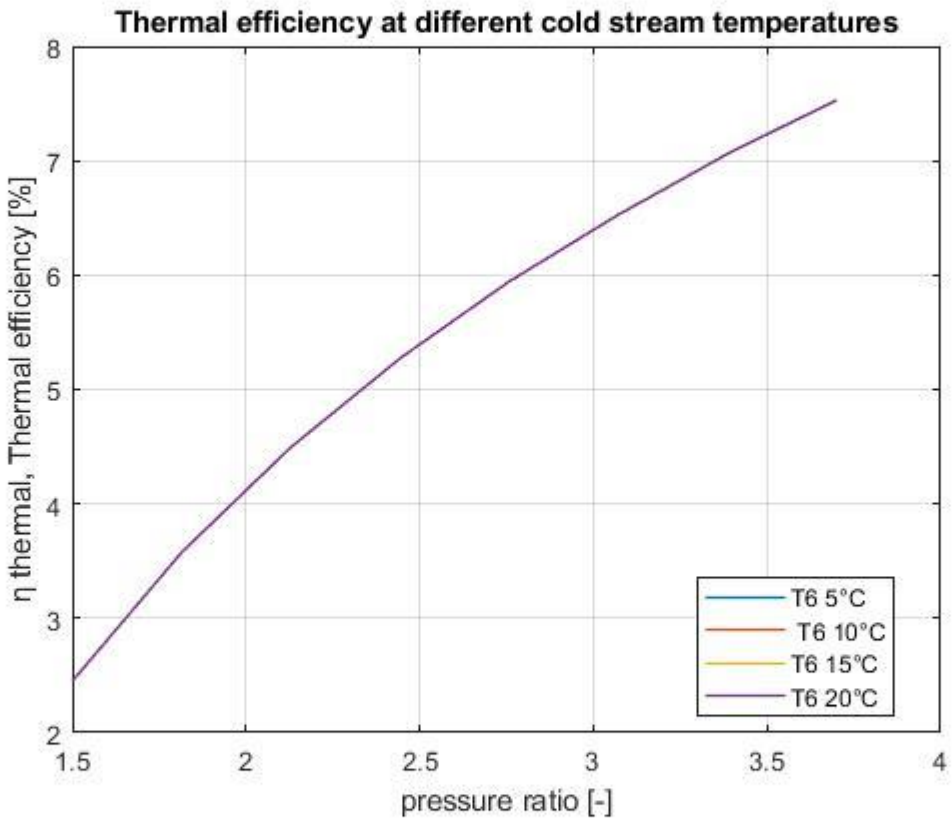

Figure 13 Thermal efficiency at different T6 and pressure ratios.

By inspecting *Figure 13,* a similar trend as found in case 1 can be identified. The thermal efficiency doesn't get affected by an increasing condenser inlet temperature but increases with an increasing rc. The thermal efficiency is higher than the system efficiency at any given rc.

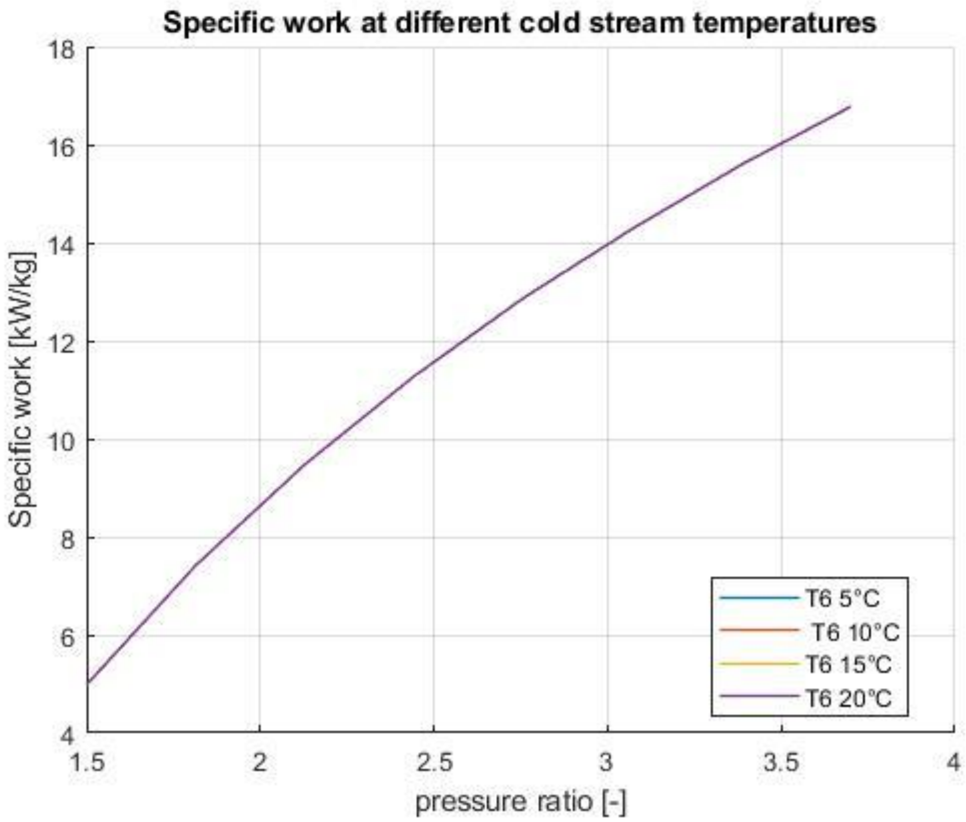

Figure 14 Specific work at different T6 and pressure ratios.

Like the thermal efficiency, the specific work is not affected by an increasing condenser temperature T_6. If the pressure ratio increases the specific work increases with no exception. This means that the primary system size decreases with an increasing pressure ratio. The secondary systems have no impact on the specific work.

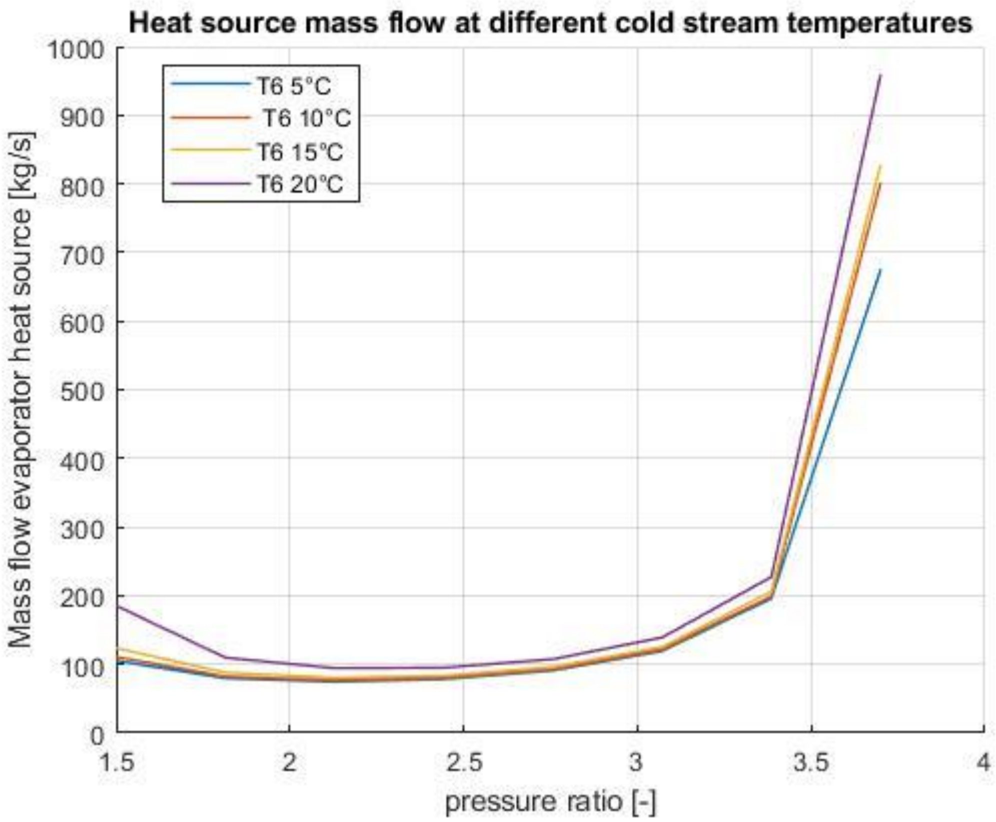

Figure 15 Evaporator mass flow at different T6 and pressure ratios.

Analysing *Figure 15* a turning point for all curves can be identified between a pressure ratio of 2 and 2.5. From rc 2.5 and onwards $\dot{m}_{s,evap}$ increases more and more as the pressure ratio increases due to a smaller temperature difference between the evaporation temperature and T_8. For a rc larger than 3.4, this temperature difference is very small thus a steep increase in the $\dot{m}_{s,evap}$. Changing T_6 from 20 to 15 °C have a positive effect on $\dot{m}_{s,evap}$, especially at low rc, where the $\dot{m}_{s,evap}$ is almost doubled at rc 1.5. Which stresses the importance of a low T_6 at low-pressure ratios. However, changing T_6 from 15 to 10 or 15 to 5 °C does not affect $\dot{m}_{s,evap}$ in a significant matter.

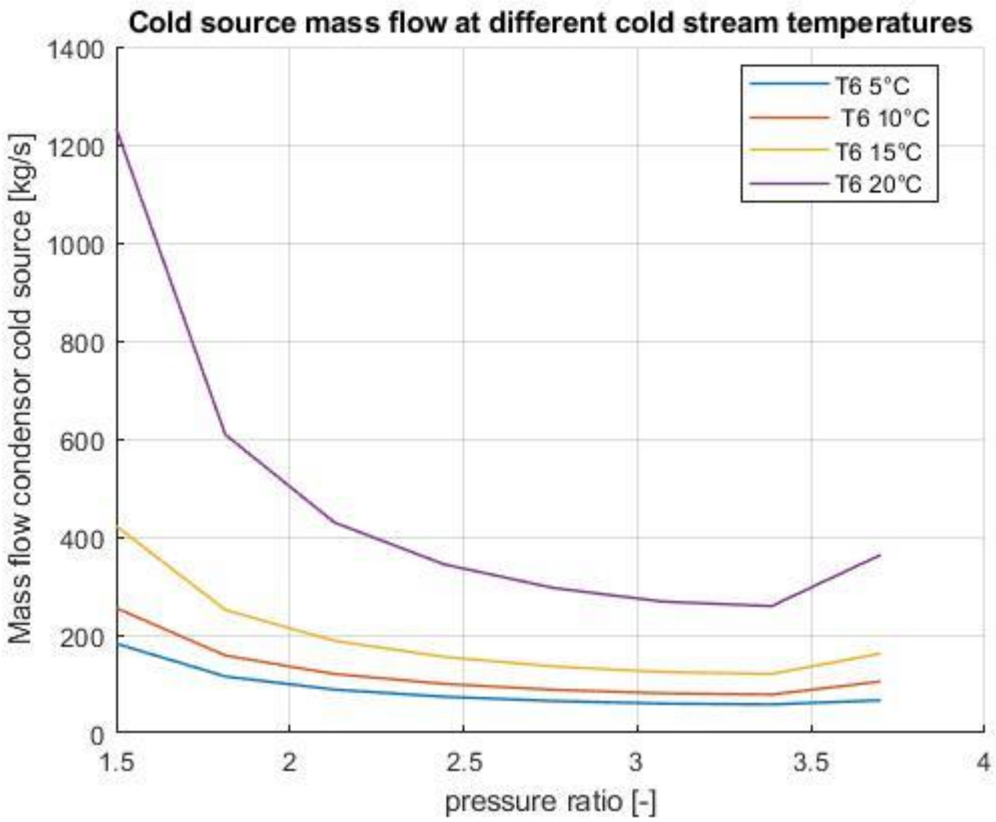

Figure 16 Condenser mass flow at different T6 and pressure ratios.

Reviewing *Figure 16* a low T_6 has a positive effect on the $\dot{m}_{s,cond}$ and thus a positive effect on the $\dot{W}_{s,cond}$. For low-pressure ratios a decrease in T_6 has a significant effect on the system and $\dot{m}_{s,cond}$ can be reduced by 6 times if T_6 is reduced from 20 to 5 °C. $\dot{m}_{s,cond}$ also decreases up until when rc reaches 3.4 where the increasing $\dot{m}_{s,evap}$ affect the whole system in a negative matter.

6 DISCUSSION

Waste heat is a large energy source found in industry, geothermal sources, and various heat loads. This waste heat can be converted to electrical energy with an ORC and thus reduce the consumption of fossil fuels, leading to less greenhouse gas emissions. It is however important to note that many organic fluids utilized in the ORC are strong greenhouse gases including the R245fa which was chosen as the working fluid in this work. So, making sure that the system is sealed properly is essential otherwise the potential greenhouse gas decrease from not using fossil fuels might be mitigated by a leaking system. The amount of heat that can be converted to electricity is only a couple of percent. But the vast waste heat asset makes it interesting to utilize. But if components, especially pumps and turbines designed for ORC applications with higher efficiencies come to market the conversion efficiency could increase quite dramatically. Working with the system should not impose any real danger to the staff, the components utilized in the system are well-developed and safe. Nor does the pressure and the heat impose any real danger, thus they are relatively low. However, systems working with higher heat source temperatures and higher pressures could be dangerous if not managed properly.

6.1 Key performance parameters and system performance

All the input variables $PPTD, T_6$ and rc can be categorized as important performance parameters for an ORC system working with a low-temperature heat stream of 80 °C. They all have a significant effect on the system's efficiency and thus the system's performance. However, $PPTD$ and T_6 have no significant effect on the specific work output of the system. But they impose a positive effect on the system efficiency and system performance when they are lowered.

A small $PPTD$ will lead to a lower mass flow required in the secondary system. A low mass flow in the secondary system means that the work consumed by the pumps decreases and thus this will lead to an increase in the system efficiency. Nonetheless, a low $PPTD$ can impose problems such as a large pressure drop due to a large heat exchanger area and costly heat exchangers to mitigate pressure losses caused by the large size. The specific work output of the primary system does not get affected by varying the $PPTD$. The specific work only analyses the primary system, so if the consumed work by the secondary system increases which $PPTD$ mostly effect this will not affect the results of the specific work. To achieve a good-performing system the $PPTD$ should be as low as possible but the pressure drop imposed by the small $PPTD$ must be considered. To find a suitable operating point for this PPTD the system efficiency can be analyzed to find a pressure ratio that achieves good efficiency.

A lower T_6 only have a positive impact on the system performance and system efficiency, causing both the secondary mass flows to decrease. But the decrease in mass flow is much more prominent in the condenser than in the evaporator, but this decrease in the secondary mass flow leads to a decrease in the work consumed by the pump thus increasing the system efficiency. It can however be challenging to find a constant low-temperature source. The temperature might also change during the year which stresses the importance of a system being able to handle an alternating temperature.

When considering rc system performance reacts positively when the pressure ratio increases, up until the point where the evaporation temperature comes close to the hot inlet temperature T_8. At some point, the temperature difference between the T_8 and the evaporation temperature becomes so low that the secondary mass flow increases dramatically thus limiting the performance.

There is however no way definitively determine which parameter is most important for the system's performance. But the pressure ratio seems to be the most impactful parameter for the performance of the system thus affecting all the performance parameters investigated in this work.

It's important to note that the pumping work in the secondary systems is the parameter that limits the system's performance and efficiency. This effect cannot be identified when reviewing the thermal efficiency and the specific work output of the system. In which nor $PPTD$ or T_6 affect the performance indicators. rc however, does affect both the thermal efficiency and the specific work but only in a positive matter. No turning points were identified for thermal efficiency or specific work which suggests that the trend will continue for higher pressure ratios.

6.2 Constraints

The main constraint identified in this work is the pressure range in which the system can operate. The upper-pressure limit in the system is constrained by the evaporation temperature. The relationship between pressure and evaporation temperature is derived from the thermodynamic properties of the working fluid. Thus, at a given pressure there is a saturated temperature/evaporation temperature for this pressure where the fluid starts to boil. The same thermodynamic relationship is found in the condenser where the lower pressure limit is constrained by the condensing temperature. So, if T_6 is higher the lower pressure limit of the cycle is constrained to a higher pressure. As can be identified by reviewing the graphs a small pressure ratio will limit the system performance. The system is also constrained by the $PPTD$ but in a more indirect way. When the $PPTD$ is 0 the heat exchangers are theoretically optimized and thus the systems achieve a higher system efficiency but a low $PPTD$ will probably affect both the cost and the pressure drop in the system in a negative matter thus constraining the system performance. A large pressure drop in the evaporator would decrease the inlet pressure entering the turbine leading to a smaller power output.

7 CONCLUSIONS

For an ORC system to achieve good system efficiency the pinch point temperature should be as small as real-world applications permit. The system should then be analyzed at this $PPTD$ to find the pressure ratio which achieves the best system performance. However, as mentioned in the discussion a low $PPTD$ will also affect the size of the heat exchange and thus pressure loss and cost.

Reviewing the results in case two the graphs suggest that T_6 should be kept as low as possible, this not only increases the system performance at any given pressure ratio. It will also allow the system to work within a larger range of pressure ratios and thus achieve a larger system efficiency and specific work. It's important to note that if T_6 could be lowered from 20 to 15 °C This will cause a larger increase in the system efficiency than if T_6 would be lowered from 15 to 10 °C.

When the pressure ratio in the system increases all the performance parameters are affected in a positive way. However, contrary to the thermal efficiency and the specific work at a certain pressure ratio the system efficiency and the secondary mass flow in the evaporator is affected negatively with an increasing pressure ratio.

Using thermal efficiency to evaluate how much of the thermal energy can be converted to electrical energy in a real-world scenario does not present a representative value. The thermal efficiency only includes primary main components with no losses. A suggestion would be to use system efficiency like this work has used to evaluate the system performance. Because this includes both the primary and secondary main components thus providing a more reliable result. However, in a real-world system, the auxiliary components would be plenty more and consume power from the system. But this work chose to focus on the main power consumers in the system and thus are included in the system efficiency.

In the table below a (+) means that the input parameter causes a positive effect on the performance parameter. A (-) sign means that the parameter has a negative effect on the parameter. For an increasing rc the performance parameters mostly react positively. However, at a certain pressure ratio the evaporation temperature comes so close to T_8 thus increasing the secondary pump work massively which has a negative effect on the performance parameters. Which is why a (-) sign has been included after a semicolon, this means at a certain pressure ratio the positive effect vanishes and a further increase in pressure ratio affect the system performance negatively.

Table 6 Displays how inputs affect performance indicators.

Input:	η_{system}	η_{th}	$\dot{W}_{spec}$	$\dot{m}_{s,condenser}$	$\dot{m}_{s,evaporator}$
$T_6, decreasing$	+			++	
$PPTD$, decreasing	++			++	+
$rc, increasing$	++ ; -	++	++	++	+ ; -

8 SUGGESTIONS FOR FURTHER WORK

8.1 Potential improvements

To enhance the quality of this work, some changes could have been made. The $PPTD$ Should have been varied in the two heat exchangers independently to see how $PPTD$ would affect the system when varied in the evaporator and then in the condenser. This would allow for another conclusion, which of the heat exchangers is most important to have a low $PPTD$. The isentropic efficiency used for the pumps was all set to the same value, but water pumps should probably have a higher isentropic efficiency than what was used. That would lead to a slightly better-performing system and thus system efficiency would increase.

Developing a model to investigate a system is always challenging and the room for error is large. The model created within the scope of this work was validated by comparing results with the literature there are still uncertainties regarding the model's performance. Two mistakes could counteract each other and cause the model to produce results that appear correct. To further validate the model and counteract uncertainties more parameters should have been analyzed and compared.

Including a high-fidelity heat exchanger model which can calculate the heat exchange area and the pressure drop as a function of the heat exchange area. This would allow for a more comprehensive review of how the system is affected by different $PPTD$. Thus, the effect of pressure loss in conjunction with the increasing area for a decreasing $PPTD$. It would also be interesting to evaluate how a restriction on the outlet temperature of the evaporator hot water fluid would constrain the system.

REFERENCES

Alvares, H. (2006). *Energiteknik* (3rd ed., Vol. 1). Studentlitteratur.

Brodal, E., Jackson, S., & Hailu, G. (2023). UA and pinch point temperature difference modeling — Finding the best heat exchanger schemes. *Computers & Chemical Engineering*, *169*, 108085. https://doi.org/10.1016/J.COMPCHEMENG.2022.108085

Canbolat, A. S., Bademlioglu, A. H., & Kaynakli, O. (2023). *Energy Sources, Part A: Recovery, Utilization, and Environmental Effects ISSN: (Print) (Online) Journal homepage: https://www.tandfonline.com/loi/ueso20 A modeling of electricity generation by using geothermal assisted organic Rankine cycle with internal heat recovery*. https://doi.org/10.1080/15567036.2019.1684598

Deethayat, T., Asanakham, A., & Kiatsiriroat, T. (2016). Performance analysis of low temperature organic Rankine cycle with zeotropic refrigerant by Figure of Merit (FOM). *Energy*, *96*, 96–102. https://doi.org/10.1016/J.ENERGY.2015.12.047

Dick, E. (n.d.). *Fluid Mechanics and Its Applications Fundamentals of Turbomachines Second Edition*. https://link.springer.com/bookseries/5980

Dixon, S. L., & Hall, C. A. (2010). *Fluid mechanics and thermodynamics of turbomachinery* (6th ed.). Burlington, Mass. : Butterworth-Heinemann/Elsevier.

Energy Agency, I. (n.d.). *Secure Sustainable Together Capturing the Multiple Benefits of Energy Efficiency*. http://www.iea.org/termsandconditionsuseandcopyright/

Feng, Y. Q., Zhang, Q., Xu, K. J., Wang, C. M., He, Z. X., & Hung, T. C. (2023). Operation characteristics and performance prediction of a 3 kW organic Rankine cycle (ORC) with automatic control system based on machine learning methodology. *Energy*, *263*. https://doi.org/10.1016/j.energy.2022.125857

Gerhart, P. M., Gerhart, A. L., & Hochstein, J. I. (2017). *Munson's Fluid Mechanics* (8th ed.). Wiley.

Granryd, E., Kungliga Tekniska högskolan. Institutionen för energiteknik, KTH Industrial Engineering and Management, & Royal Institute of Technology, KTH. D. of E. T. (2009). *Refrigerating engineering*. Royal Institute of Technology, KTH, Department of Energy Technology, Division of Applied Thermodynamics and Refrigeration.

Hu, B., Guo, J., Yang, Y., & Shao, Y. (2022). Selection of working fluid for organic Rankine cycle used in low temperature geothermal power plant. *Energy Reports*, *8*, 179–186. https://doi.org/10.1016/j.egyr.2022.01.102

Huo, D., Tian, H., Shu, G., & Wang, W. (2022). Progress and prospects for low-grade heat recovery electrochemical technologies. In *Sustainable Energy Technologies and Assessments* (Vol. 49). Elsevier Ltd. https://doi.org/10.1016/j.seta.2021.101802

Huo, D., Tian, H., Wang, W., & Shu, G. (2022). Enhancing heat-to-electricity conversion performance of the thermally regenerative electrochemical cycle using carbon-copper composite electrodes. *Sustainable Energy Technologies and Assessments*, *53*. https://doi.org/10.1016/J.SETA.2022.102793

Imran, M., Usman, M., Park, B. S., Kim, H. J., & Lee, D. H. (2015). Multi-objective optimization of evaporator of organic Rankine cycle (ORC) for low temperature geothermal heat source. *Applied Thermal Engineering*, *80*, 1–9. https://doi.org/10.1016/j.applthermaleng.2015.01.034

Incropera, F. P., & DeWitt, D. P. (2002). *Fundamentals of heat and mass transfer* (5th ed.).

Jouhara, H., Khordehgah, N., Almahmoud, S., Delpech, B., Chauhan, A., & Tassou, S. A. (2018). Waste heat recovery technologies and applications. In *Thermal Science and Engineering Progress* (Vol. 6, pp. 268–289). Elsevier Ltd. https://doi.org/10.1016/j.tsep.2018.04.017

Kaya, A., Lazova, M., Bağcı, Ö., Lecompte, S., Ameel, B., & De Paepe, M. (2017). Design Sensitivity Analysis of a Plate-Finned Air-Cooled Condenser for Low-Temperature Organic Rankine Cycles. *Heat Transfer Engineering*, *38*(11–12), 1018–1033. https://doi.org/10.1080/01457632.2016.1216966

Kim, D. K., Lee, J. S., Kim, J., Kim, M. S., & Kim, M. S. (2017). Parametric study and performance evaluation of an organic Rankine cycle (ORC) system using low-grade heat at temperatures below 80 °C. *Applied Energy*, *189*, 55–65. https://doi.org/10.1016/j.apenergy.2016.12.026

Lecompte, S., Huisseune, H., Van Den Broek, M., Vanslambrouck, B., & De Paepe, M. (2015). Review of organic Rankine cycle (ORC) architectures for waste heat recovery. In *Renewable and Sustainable Energy Reviews* (Vol. 47, pp. 448–461). Elsevier Ltd. https://doi.org/10.1016/j.rser.2015.03.089

Li, H., Liu, C., Xu, Z., Liu, J., Du, Z., Li, M., Dong, J., Han, Z., Xu, M., & Pan, X. (2023). Performance comparison of thermal power generation-organic Rankine cycle combined cycle system for ships waste heat utilization under different bottom cycle ratios. *Environmental Progress and Sustainable Energy*, *42*(2). https://doi.org/10.1002/ep.13993

Moran, M. J., Shapiro, H. N., Boettner, D. D., & Bailey, M. B. (n.d.). *FUNDAMENTALS OF ENGINEERING THERMODYNAMICS Eighth Edition*. www.wiley.com/college/moran.

Naas, T. T., Telha, M., Laib, L., Shakhawat, H., Bacha, A., Taibaoui, A., Naas, A. Z., & Aissaoui, D. (2021). Performance enhancement of three-stage axial turbine for Clean Organic Rankine Cycle system driven by low-temperature heat source. *Cleaner Engineering and Technology*, *5*. https://doi.org/10.1016/j.clet.2021.100336

Normal årsmedeltemperatur | SMHI. (n.d.). Retrieved May 18, 2023, from https://www.smhi.se/data/meteorologi/temperatur/normal-arsmedeltemperatur-1.3973

R-245fa is a hydrofluorocarbon HFC, refrigerant. (n.d.). Retrieved April 27, 2023, from https://climalife.dehon.com/r-245fa

Refrigerant Product Range - TEGA. (n.d.). Retrieved April 27, 2023, from https://www.tega.de/en/products/refrigerants/products

Wang, S., Liu, C., Li, Q., Liu, L., Huo, E., & Zhang, C. (2020). Selection principle of working fluid for organic Rankine cycle based on environmental benefits and economic performance. *Applied Thermal Engineering*, *178*. https://doi.org/10.1016/j.applthermaleng.2020.115598

Water (data page) - Wikipedia. (n.d.). Retrieved April 27, 2023, from https://en.wikipedia.org/wiki/Water_(data_page)

Xia, J., Wang, J., Wang, H., & Dai, Y. (2018). Three-dimensional performance analysis of a radial-inflow turbine for an organic Rankine cycle driven by low grade heat source. *Energy Conversion and Management*, *169*, 22–33. https://doi.org/10.1016/j.enconman.2018.05.038

Yang, Y., Zhang, H., Xu, Y., Yang, F., Wu, Y., & Lei, B. (2018). Matching and operating characteristics of working fluid pumps with organic Rankine cycle system. *Applied Thermal Engineering*, *142*, 622–631. https://doi.org/10.1016/j.applthermaleng.2018.07.039

Zare, V. (2015). A comparative exergoeconomic analysis of different ORC configurations for binary geothermal power plants. *Energy Conversion and Management*, *105*, 127–138. https://doi.org/10.1016/j.enconman.2015.07.073